Journal of South American Earth Sciences 29 (2010) 832–848

Contents lists available at ScienceDirect

Journal of South American Earth Sciences

journal homepage: www.elsevier.com/locate/jsames

Clockwise rotation of the Santa Marta massif and simultaneous Paleogene to Neogene deformation of the Plato-San Jorge and Cesar-Ranchería basins

Camilo Montes [a,*], Georgina Guzman [b], German Bayona [c], Agustin Cardona [a], Victor Valencia [d], Carlos Jaramillo [a]

[a] Smithsonian Tropical Research Institute, Unit 9100, Box 0948, DPO AA 34002-9998, USA
[b] Invemar, Cerro Punta Betín, Santa Marta, AA 1016, Colombia
[c] Corporación Geológica Ares, Calle 57 # 23-09, Bogotá, Colombia
[d] Arizona Lasechron Center, The University of Arizona, Tucson AZ, USA

ARTICLE INFO

Article history:
Received 9 December 2008
Accepted 21 July 2009

Keywords:
Tectonics
Rotation
Northern Colombia
Santa Marta
Cerrejon
Perija
Plato
San Jorge
Paleomagnetism
Geochronology

ABSTRACT

A moderate amount of vertical-axis clockwise rotation of the Santa Marta massif (30°) explains as much as 115 km of extension (stretching of 1.75) along its trailing edge (Plato-San Jorge basin) and up to 56 km of simultaneous shortening with an angular shear of 0.57 along its leading edge (Perijá range). Extensional deformation is recorded in the 260 km-wide, fan-shaped Plato-San Jorge basin by a 2–8 km thick, shallowing-upward and almost entirely fine-grained, upper Eocene and younger sedimentary sequence. The simultaneous initiation of shortening in the Cesar-Ranchería basin is documented by Mesozoic strata placed on to lower Eocene syntectonic strata (Tabaco Formation and equivalents) along the northwest-verging, shallow dipping (9–12° to the southeast) and discrete Cerrejón thrust. First-order subsidence analysis in the Plato-San Jorge basin is consistent with crustal stretching values between 1.5 and 2, also predicted by the rigid-body rotation of the Santa Marta massif. The model predicts about 100 km of right-lateral displacement along the Oca fault and 45 km of left-lateral displacement along the Santa Marta–Bucaramanga fault. Clockwise rotation of a rigid Santa Marta massif, and simultaneous Paleogene opening of the Plato-San Jorge basin and emplacement of the Cerrejón thrust sheet would have resulted in the fragmentation of the Cordillera Central–Santa Marta massif province. New U/Pb ages (241 ± 3 Ma) on granitoid rocks from industry boreholes in the Plato-San Jorge basin confirm the presence of fragments of a now segmented, Late Permian to Early Triassic age, two-mica, granitic province that once spanned the Santa Marta massif to the northernmost Cordillera Central.

1. Introduction

The Santa Marta massif is located along the diffuse southern Caribbean plate boundary (Fig. 1), a margin owing its character to the oblique convergence and right-lateral shearing between the Caribbean plate and northwestern South America (Pindell et al., 1998; Moreno and Pardo, 2003; Kennan and Pindell, in press). The Santa Marta massif is flanked on two of its sides by sedimentary basins with contrasting structural styles and sedimentary fills. The Plato-San Jorge basin is a multi-compartment basin that contains a mostly undeformed (Flinch, 2003), 2–8 km-thick, paralic and marine upper Eocene to Pliocene sequence (Duque-Caro, 1979; Rincón and Arenas, 2007); it lies west of the massif in tectonic contact along the Santa Marta–Bucaramanga fault (Campbell, 1965). Southeast of the massif is the Cesar-Ranchería basin, a non-faulted basin that preserves a ~2 km-thick clastic wedge that records marine to continental, Late Cretaceous to Neogene sedimentation (Bayona et al., 2007; Ayala, 2009). This clastic wedge developed on the southeastern flank of the Santa Marta massif and is now bound by the Cerrejón thrust sheet to the southeast (Kellogg, 1984).

General similarities in lithology and structural style between the Santa Marta massif–Cesar-Ranchería basin pair to the north, and the northern Cordillera Central–middle Magdalena basin pair to the south, led previous workers to suggest that these basin/range pairs were adjacent and later became tectonically segmented during tertiary times either by vertical-axis rotation of the Santa Marta massif block (~34°, Duque-Caro, 1979; Reyes et al., 2000; Hernandez and Ramirez, 2003; Hernandez et al., 2003; Montes, 2003) or by left-lateral displacement along the Santa Marta–Bucaramanga fault (110 km, Campbell, 1965). Nonetheless, modern tectonic reconstructions have considered the evolution of these blocks in a more static (Villamil, 1999; Cediel et al., 2003), or orthogonal manner (Gómez et al., 2005; Pindell and Keenan,

* Corresponding author. Tel.: +1 507 212 8090.
E-mail address: montesc@si.edu (C. Montes).

0895-9811/$ - see front matter © 2009 Elsevier Ltd. All rights reserved.
doi:10.1016/j.jsames.2009.07.010

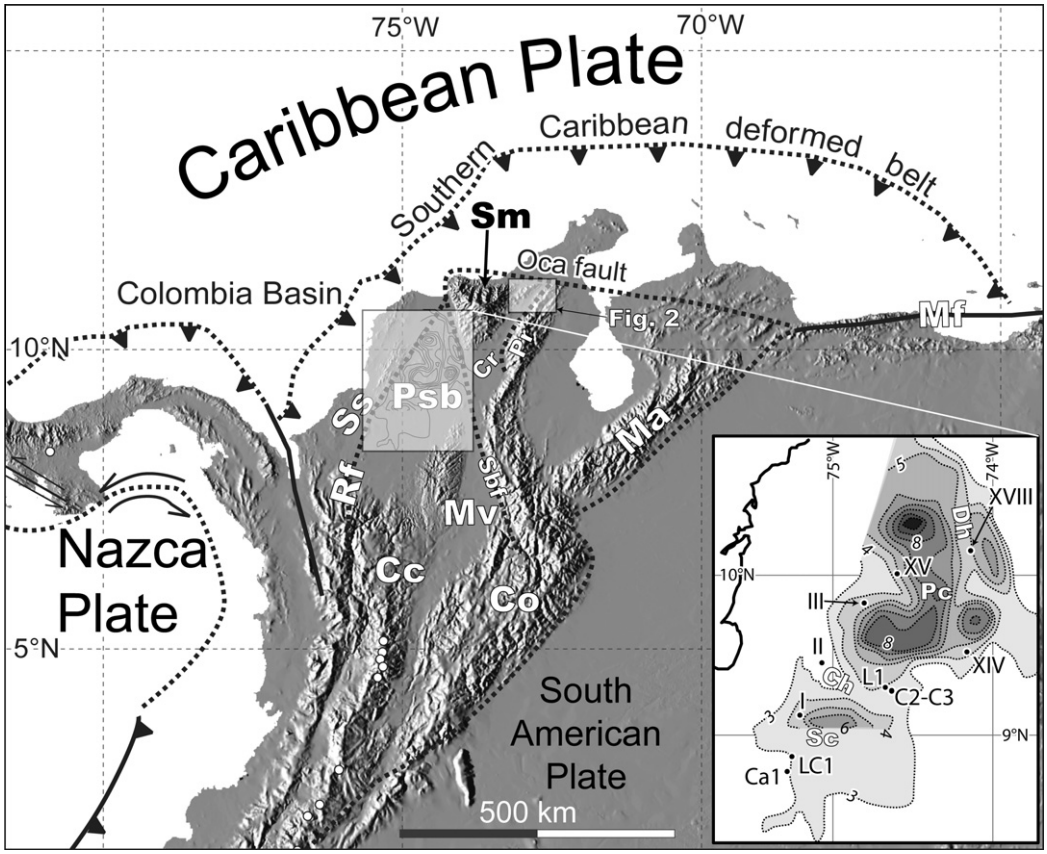

Fig. 1. Tectonic setting of the Santa Marta massif and surrounding Cesar-Ranchería and Plato-San Jorge basins. Sbf, Santa Marta–Bucaramanga fault; Cc, Cordillera Central; Co, Cordillera Oriental; Cr, Cesar-Ranchería basin; Ma, Mérida Andes; Mv, middle Magdalena valley; Mf, Morón fault system; Psb, Plato-San Jorge basin; Pr, Perijá range; Sm, Santa Marta massif; Ss, Sinu-San Jacinto deformed belts; Rf, Romeral fault zone. Modified from Burke et al. (1978), and Burke et al. (1984), Mann and Burke (1984). Inset shows depth to basement in the Plato-San Jorge basin in km below surface (Cerón et al., 2007). Roman numerals represent boreholes from Rincón et al. (2007). Ca1, Cabanos-1; Ch, Cicuco high; Dh, Dificil high; LC1, Los Cayos-1; C2–C3, Cicuco 2 and 3; L1, Lobita-1; Pc, Plato compartment; Sc, Sucre compartment.

2001). Another approach to the dynamics of this margin was postulated by Montes et al. (2005a) considering the possibility of vertical-axis rotation of the Maracaibo block.

In this paper, we build on previous reconstructions (Campbell, 1965; Duque-Caro, 1979; Montes et al., 2005a) by solving the simultaneous extensional and compressional deformation along the western and southeastern flanks of the Santa Marta massif. We propose that clockwise, vertical-axis rotation of the massif would simultaneously open up accommodation space in the Plato-San Jorge basin while shortening the Cesar-Ranchería basin. This model explains the coupled evolution of contrasting structural styles found today on two of the flanks of the Santa Marta massif while maintaining kinematic compatibility.

Three lines of evidence are interwoven here to refine previous models. They are: (1) new structural mapping that documents early Eocene and younger shortening along the western foothills of the Perijá range; (2) new stratigraphic sections measured in the western edge of the Plato basin (Guzman, 2007) and existing biostratigraphic zonations based on industry borehole information (Rincón et al., 2007; Cuartas et al., 2006) that record post-late Eocene basin opening and extension in the Plato-San Jorge basin, and (3) new geochronological data from basement rocks recovered from industry borehole cores in the Plato basin that suggests a once continuous Permo-Triassic magmatic belt spanning the Santa Marta massif, the Plato-San Jorge basin and the northern Cordillera Central. This information is complemented with new paleomagnetic data in the stable core of the Santa Marta massif (Bayona et al., this issue) and published industry geophysical data (Flinch, 2003; Cerón et al., 2007). The resulting model suggests that moderate amounts of vertical-axis, clockwise rotation of the Santa Marta massif can simultaneously solve approximately 100 km of extension along its trailing edge (Plato-San Jorge basin) and about 100 km of oblique shortening along its leading edge (Perijá range).

2. Geologic setting

The Santa Marta massif is a topographic high isolated from all other mountain massifs and ranges of the northern Andes. All its bounding structures also represent major structures along the southern Caribbean plate boundary. They include the right-lateral Oca fault (Irving, 1971), the left-lateral Santa Marta–Bucaramanga fault (Campbell, 1965), the Cerrejón thrust (Kellogg, 1984), and the Romeral suture (Fig. 1). Two basins surround the Santa Marta massif: the Plato-San Jorge basin to the west and the Cesar-Ranchería basin to the southeast; the former in tectonic contact with the massif, the latter in structural continuity with it. Both the Santa Marta and Oca faults have been characterized primarily as strike-slip faults based on lithological piercing-points. Both these faults, however, also have a very large vertical component around the Santa Marta massif, as it is easily deduced from simple comparison of basement depths on both sides of each fault. The Santa Marta massif exposes its crystalline basement at heights of up to 5 km, while the basins immediately to its west (Plato compartment) and north (baja Guajira) have a sedimentary cover as thick as 8 km in the Plato compartment (Duque-Caro, 1979) and as thick as 3 km in baja Guajira (Rincón et al., 2007).

2.1. Plato-San Jorge basin

Two main compartments (Plato and Sucre) separated by the northwest-trending Cicuco high, make up the Plato-San Jorge basin (Duque-Caro, 1979). To the east, the north-trending Dificil high separates the Plato basin from a deep and narrow compartment next to the Santa Marta massif. Further east, the Santa Marta–Bucaramanga fault marks the eastern boundary of the Plato-San Jorge basin. Its western border is defined by the Romeral fault and the Sinu-San Jacinto deformed belt. To the south, its border is indistinct against the northern foothills of the Cordillera Central (Fig. 1). Oil industry data (Duque-Caro, 1979; Flinch, 2003; Cerón et al., 2007) indicate that an approximately 3 km-thick, flat-lying, lower Oligocene to Recent sedimentary sequence (Duque-Caro, 1979; Cuartas et al., 2006; Rincón and Arenas, 2007) covers the Cicuco and Dificil highs, while a much thicker (up to 8 km), and slightly older sequence is preserved within the Plato and Sucre compartments. Turbidites are present within both compartments, but absent in the highs, leading Duque-Caro (1979) to propose that the compartments behaved as submarine canyons during the Neogene.

Basement of the Plato-San Jorge basin is extended continental crust, as demonstrated by geophysical and borehole data (Cerón et al., 2007). Existing geochronological data in basement rocks in the Plato-San Jorge basin include a ca. 110 Ma biotite K–Ar obtained in a biotite granitoid from the Cicuco-3 well (Pinson and Hurley, 1962), and several ca. 110 Ma and 60 Ma Rb–Sr, K–Ar ages from low-grade schist and a volcanic rock of the El Cabano-1 and Los Cayos-1 wells (Thery et al., 1977). The K–Ar biotite samples obtained by Thery et al. (1977) could represent either a partial or a total resetting ages recording cooling to 250 °C, event since the rocks analyzed are in the greenschist facies. The age obtained from volcanic rocks in the Los Cayos-1 well may record a magmatic event of this age. Although these ages have counterparts in the Cordillera Central (Thery et al., 1977; Toussaint, 1996), they also overlap with magmatic and metamorphic episodes within the allochthonous Caribbean fragments (reviews in Pindell and Kennan, 2001).

2.2. Cesar-Ranchería basin

The Cesar-Ranchería basin preserves an Upper Cretaceous to Paleogene clastic wedge in the southeastern dip-slope of the Santa Marta massif. Detailed studies of this Paleogene sedimentary wedge indicate tilting and unroofing of the massif during Paleocene times (Bayona et al., 2007), a consequence of its collision with the Caribbean deformation front and accretion of a Paleocene arc (Cardona et al., in press). This collision would have tilted the northwestern corner of the massif thus opening accommodation space inboard along its southeastern flank, where accumulation of the coal-bearing Cerrejón Formation took place (Montes et al., 2005b).

Detailed petrographic, provenance, paleocurrent and sedimentological analyses in the Paleocene Cerrejón Formation in the northernmost part of the Cesar-Ranchería valley indicate that clastic material making up the bulk of the more than 1500 m thick Manantial and Cerrejón Formations had the Santa Marta massif as a source area (Bayona et al., 2007; Ayala, 2009). Clastic components include microcline, graphitic schist, mica schist, unzoned garnets and high-temperature biotite, consistent with a source in the Santa Marta massif, and not the Perijá range. This thick synorogenic sedimentary wedge thickens southeastward up to 2.2 km and increases its K-feldspar and quartz content to the top (Tabaco formation), indicating that tectonic activity in the Perijá range began during Eocene times (Bayona et al., 2007; Cardona et al., in press; Ayala, 2009).

3. Shortening in the Cesar-Ranchería basin

Structures accommodating large contractional strains have long been recognized and mapped along the foothills of the Perijá range (Kellogg and Bonini, 1982; Kellogg, 1984; Duerto et al., 2006). The structure of this range is dominated by the northwest-verging Cerrejón thrust along its western flank, the southeast-verging Motilones fault system along its southeastern flank, and the Tigre fault along the axis of the range (dextral strike-slip according to Duerto et al., 2006 or northwest-verging according to Kellogg, 1984). Early Eocene (53 Ma), middle Eocene (45 Ma) and late Oligocene (25 Ma) unconformities reported in the eastern flank of the Perijá range indicate that mild deformation started during early Eocene times and was more intense during late Oligocene times with thrust sheet emplacement where 3–4 km unroofing of thrust sheets took place (Kellogg, 1984). Thickness changes of upper Paleogene strata along the eastern flank of the Perijá range also suggest that timing of deformation associated to the Motilones thrust was Oligocene (Duerto et al., 2006).

3.1. Structural style of the northern Cesar-Ranchería basin

The northern segment of the Cesar-Ranchería basin is defined by a southeast-dipping monocline that maintains structural continuity with the Santa Marta massif (Fig. 2). This monocline is bound to the north by the right-lateral Oca fault and to the southeast by the northwest-verging Cerrejón thrust. To the south, a series of northwest-verging thrust faults disrupt the stratigraphically higher levels of the monocline, and generate a large scarp that is buried under more than 50 m of alluvial cover, getting progressively thicker to the south. Deformation throughout the northern part of the Cesar-Ranchería valley is localized along the Cerrejón thrust, following a detachment level along incompetent strata of the Palmito Formation overlying the more competent Tabaco Formation (Fig. 3). Deformation in the footwall of the Cerrejón fault is limited to faults and folds affecting the Cerrejón Formation, including large structures such as the Ranchería fault and the Tabaco anticline, but never involving rocks below the Cerrejón Formation. Further northwest, and stratigraphically lower, there is no significant deformation in the footwall of the Cerrejón thrust, with the Cerrejón Formation resting in structural continuity on Cretaceous and Jurassic strata of the southeastern dip-slope of the Santa Marta massif (Fig. 3).

The Cerrejón fault is very well exposed along the Palomino creek canyon and the Majaguita mountain (inset in Fig. 2 and Fig. 4), where detailed geologic mapping documents thrusting of Mesozoic rocks, usually the Cretaceous Cogollo Group, on to lower Eocene rocks of the Tabaco and Palmito Formations, separated by a fault zone of no more than 20 m of breccia, and dipping only 9–12° to the southeast. The hanging wall of the Cerrejón fault is burnt as coal seams in the footwall spontaneously combusted after emplacement. Stratigraphic separation between the Cretaceous Cogollo Group and the Eocene Palmito Formation is at least 2 km (Bayona et al., 2007), and the total throw of the fault was estimated between 16 and 26 km by Kellogg and Bonini (1982).

3.2. Age of syntectonic deposits

The Tabaco Formation rests conformably on the Cerrejón Formation around the axial zone of the Tabaco anticline, but it is missing to the south, and only reappears near the Ranchería fault. In the central part of the Ranchería valley, the Eocene Palmito Formation directly rests on the Paleocene Cerrejón Formation (Fig. 2). These observations, along with provenance analyses (Bayona et al., 2007) indicate that mild deformation was already beginning to

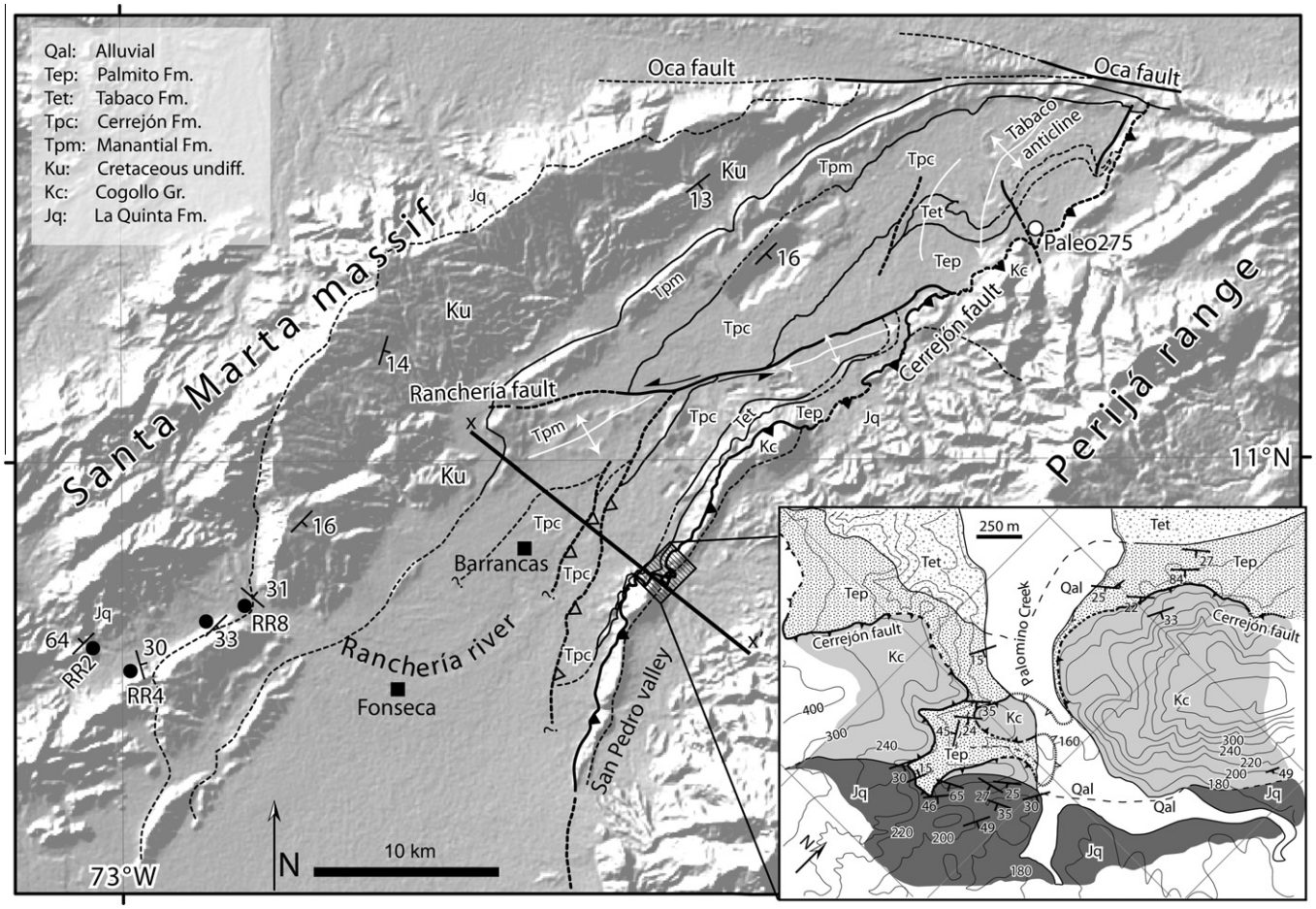

Fig. 2. Geologic map of the northern Cesar-Ranchería basin. Note how the Paleogene deposits of the Manantial, Cerrejón and Tabaco Formations rest in structural continuity on the southeastern dip-slope of the Santa Marta massif. Modified from Tschanz et al. (1974), Olivella (2005), Ruiz (2006), Palencia (2007), Sánchez (2008), Espitia (2008) and mapping by the authors. Topography from Nasa SRTM30. Inset shows geologic map of the Palomino creek canyon.

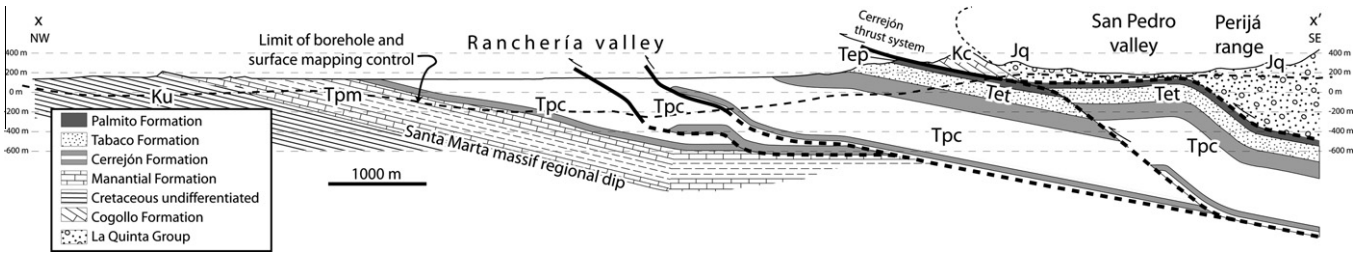

Fig. 3. Cross-section of the Cesar-Ranchería basin showing the Cerrejón Formation resting on to the southeastern dip-slope of the Santa Marta massif, and the Cerrejón thrust placing Mesozoic strata on to Paleogene strata. Location in Fig. 2. Modified from Olivella (2005), Ruiz (2006), Palencia (2007), Sánchez (2008), Espitia (2008).

Fig. 4. Panoramic view of the southern face of the Palomino creek canyon showing the topographic contrast between the Cogollo Group limestone and the underlying Palmito and Tabaco Formations.

take place in the Cesar-Ranchería basin during the accumulation of the Tabaco Formation. Similar relationships have been reported to the south (Ayala, 2009), where the equivalent of the Cerrejón Formation (Cuervos Formation) is overlain by a discontinuous unit equivalent to the Tabaco Formation (La Loma informal unit), containing detrital zircons as young as 50 Ma.

The Tabaco Formation sandstone contains magmatic zircons as young as 56 Ma (Cardona et al., in press), clearly constraining its age to be early Eocene or younger. Biostratigraphic zonations (Jaramillo et al., 2007) confirm that the underlying Cerrejón Formation spans from the middle to the late Paleocene. A single sample of a black shale of the overlying Palmito Formation (Fig. 2, sample Paleo275) contains an assemblage that is characteristic of the pollen zone T-05 of Jaramillo et al. (2009), or pollen zone 17 of Muller et al. (1987) that have been calibrated as Lower Eocene (Muller et al., 1987; Jaramillo et al. 2009). The palynological sample is composed by a rich palynoflora composed of *Polypodiisporites* sp., *Mauritiidites franciscoi* minutus, *Mauritiidites franciscoi franciscoi*, *Mauritiidites franciscoi pachyexinatus*, *Polypodiisporites* aff. *specious*, *Cyclusphaera scabrata*, *Retitrescolpites*? *irregularis*, *Retibrevitricolporites* sp., *Psilatriletes* sp., *Monocolpopollenites ovatus*, Tetracolporopollenites sp., *Retitrescolpites baculatus*, *Clavatricolpites densiclavatus*, *Poloretitricolpites absolutus*, *Longapertites proxapertitoides reticuloides*, *Laganiopollis crassa*, *Margocolporites* sp., and *Bombacacidites* sp.

The Tabaco Formation and its equivalents to the southwest (La Loma informal unit) contain the record of the first tectonic activity in the Perijá range in the form of increased K-feldspar and quartz content (Bayona et al., 2007; Ayala, 2009) and by their discontinuous map distribution (Fig. 2). Its age is early Eocene, as constrained by detrital zircon geochronology (Cardona et al., in press; Ayala, 2009) and by the pollen content of the overlying Palmito Formation (sample 275, Fig. 2), and the underlying Cerrejón Formation (Jaramillo et al., 2007). An early Eocene initiation of mild deformation and unroofing of the Perijá range coincide with previous observations along the eastern flank of the range (Kellogg, 1984; Duerto et al., 2006), and marks the time of first activity along the Cerrejón thrust. Final emplacement of the Cerrejón thrust sheet must have taken place during late Oligocene times, as inferred from syntectonic strata in the eastern flank of the Perijá range. Late Miocene deposits in the southern part of the Cesar-Ranchería basin bracket the age of deformation (Ayala, 2009).

4. Extension

To better constrain the history recorded in the sedimentary pile of the Plato-San Jorge basin, the most complete stratigraphic section of the Plato-San Jorge basin was sought, scouting out stratigraphic sections near the Carmen-Zambrano road where sampling had taken place in the past to build biostratigraphic zonations (Petters and Sarmiento, 1956). Only the northwestern edge of this basin contains exposures suitable for stratigraphic observations, where deformation related to the Romeral fault zone folds and tilts strata, elsewhere, the flat-lying sedimentary pile can only be studied from industry borehole data, discussed below.

Published sampling sites (Petters and Sarmiento, 1956) were revisited, measured again and complemented with reference sections. Four stratigraphic sections, the El Carmen-Zambrano section (including the Alférez Creek), San Jacinto, Salvador and El Guamo Creeks were selected to define a composite stratigraphic section (Fig. 5) that represents the stratigraphy of the lower Miocene to the lower Pliocene interval in the area (Guzmán, 2007). The El Carmen-Zambrano section is the only one of these four sections that includes an almost complete sequence of this interval while the remaining three sections, the San Jacinto, Salvador and El Guamo Creek, the middle to lower Pliocene interval is not exposed.

Petters and Sarmiento (1956) described the biostratigraphy of the El Carmen-Zambrano area, creating a zonation based on samples collected by W.E. Denton along the El Carmen-Zambrano road. No formational names were used nor were rock units referenced or sections measured in those studies. The El Carmen-Zambrano road section, despite being the least continuously exposed, is stratigraphically the most complete. later, DePorta (1962) and Stone (1968) discussed the distribution of Oligocene rocks proposed by Petters and Sarmiento (1956), warning of possible re-working of biostratigraphic material. Duque-Caro (1975) describes the reworking and proposes an age younger than Oligocene and early Miocene for the *Planulina karsteni* zones overlying the Rancho Formation.

4.1. Stratigraphy of Plato basin

Strata exposed along the western edge of the Plato basin is a mostly Neogene, more than 2 km-thick, punctuated shallowing-upwards and almost entirely fine-grained, clastic sequence. This sequence is made up from bottom to top of longitudinal bars (Alférez Formation) laterally adjacent to delta plain deposits (Mandatú Formation), sheltered bays or lagoons, near a muddy delta mouth (Jesús del Monte Formation), and tidal flats and tidal channel deposits (Zambrano Formation). The total absence of conglomerates and near complete absence of carbonates indicates that the Plato basin was an area that received abundant clastic input at high sedimentation rates from distant sources. The Alférez Formation represents laterally variable wave-dominated delta and prodelta deposits that developed on a wide platform environment with longitudinal bars. Sporadic turbidite currents bring carbonate clasts with glauconite towards the top of this unit. The Mandatú Formation starts shallow and becomes deeper towards the top, grading from intertidal mudstone-dominated deposits (delta front) to very fine grained mudstone with slumping structures. The Jesús del Monte Formation also starts shallow at the base with minor variations and developing paleosols with desiccation cracks at the top, indicating a shallower delta facies. The Zambrano Formation contains continental deposits, and transitional environments and swamps (Fig. 5). Although mostly undeformed, the stratigraphy described here spans a fundamental crustal boundary: the Romeral suture. Thus, it is possible that older strata, such as the 1.5 km-thick El Carmen Formation (recording water depths between 200 and 900 m) may have been tectonically juxtaposed to the western edge of the Plato basin prior to the establishment of the thick aggradational delta.

4.2. Subsidence history

Here, we use Rincón et al. (2007) biostratigraphic and depth data from six wells (I, II, III, XIV, XV, and XVIII, Fig. 1) as well as the thicknesses, ages and sedimentological interpretations derived from the Carmen-Zambrano stratigraphic section (Table 1, Fig. 5) in an attempt to extract a first-order lithospheric stretching (McKenzie, 1978) estimate for the Plato-San Jorge basin. Rincón et al. (2007) established a biostratigraphic zonation after examining a large quantity of planktonic foraminifera samples from oil-company drilling data, defining thirteen zones and eight subzones for the Eocene to Pliocene interval. Three zones and two subzones were defined for the Eocene, three zones for the Oligocene, six zones and six subzones for the Miocene, and one zone for the Pliocene. This zonation revealed three unconformities: (1) a late Eocene–early Oligocene hiatus; (2) a late Oligocene–early Miocene hiatus; and (3) a late Miocene hiatus.

The boreholes chosen from Rincón et al. (2007) to extract subsidence information were drilled in the Plato-San Jorge basin far removed from the Romeral fault zone, crossing an undeformed,

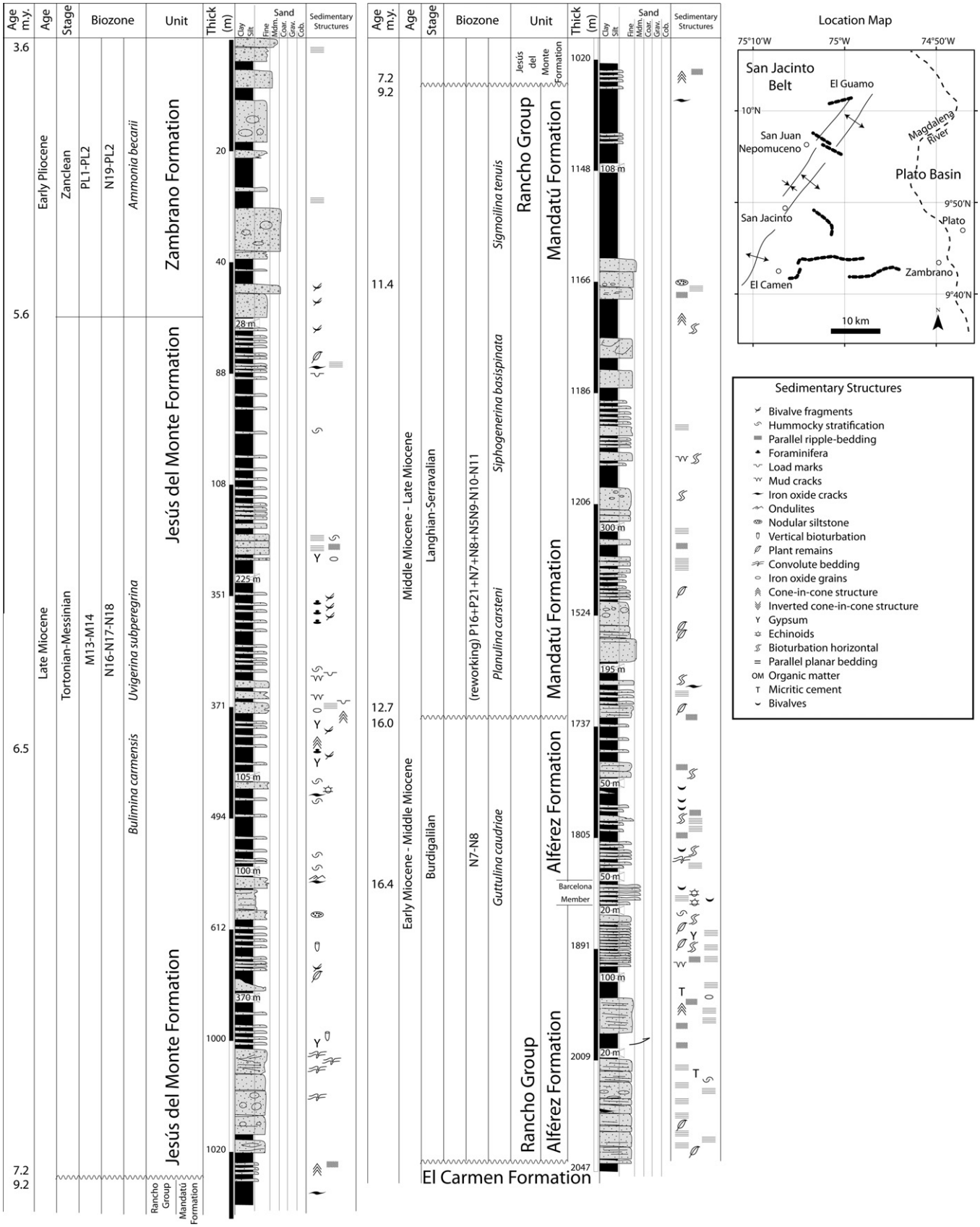

Fig. 5. Stratigraphic column of the Carmen-Zambrano road complemented with reference sections along the Alférez, San Jacinto, Salvador and El Guamo Creeks.

flat-lying (Flinch, 2003) Neogene sequence. The sedimentary pile in each well was removed using one-dimensional Airy model with exponential reduction of porosity, assuming flat dips, a mantle density of 3.3 gr/cm^3, and decompacting using the best-fit density curve derived from drilling data for the Plato basin (Cerón et al., 2007). The choice of an Airy, one-dimensional model of isostasy

Table 1
Subsidence data extracted from Rincón et al. (2007) and the stratigraphic column.

	Source	Unit name/ biozone	Base depth (km)	Age base (Ma)	Density (kg/m3)	Total subsidence (km)	Sea Level at base (km), Haq, et al. (1987)	Tectonic subsidence (km) corr. for sea level
	SS	Alferez	1.86	16.4	2200	0.17	0.14	0.01
		Unconformity	1.74	16	0	0.17		0.01
		MandatuA	1.74	12.7	2100	0.83	0.1	0.7
		MandatuB	1.17	11.4	2100	0.97	−0.08	0.73
		Unconformity	1.03	9.2	0	0.97	−0.04	0.79
		JesusA	1.03	7.2	2000	1.55	−0.08	1.1
		JesusB	0.38	6.5	1900	1.83		1.28
		Zambrano	0.04	5.6	1900	1.86	0.01	1.32
Rincón et al. (2007)	Bh I	6	3.44	27.2	2360	0.82	0.1	0.35
		7a	2.83	23.6	2360	0.85	0.12	0.48
		7b	2.8	20.3	2350	1.27	0.05	0.6
		8a	2.44	19.5	2350	1.47	0.14	0.72
		8b	2.26	16.5	2340	1.56	0.14	0.75
		9a	2.16	15.9	2020	3.05	0.13	1.88
	Bh II	7b	3.26	20.3	2340	0.83	0.05	0.34
		8a	2.65	19.5	2340	0.95	0.14	0.43
		8b	2.53	16.5	2340	1.12	0.14	0.53
		9a	2.41	15.9	2310	1.8	0.13	1.06
		9b	1.77	12.2	2200	3.21	0.05	2.1
	Bh III	3	1.22	36.8	2200	0.52	0.17	0.12
		4	0.76	33.5	2100	0.59	0.17	0.41
		5	0.7	31.3	2070	0.8	0	0.41
		6	0.49	27.2	2030	1.15	0.1	0.63
		7a	0.09	23.6	2000	1.22	0.12	0.8
	Bh XV	8b	3.75	16.5	2350	1	0.14	0.46
		9a	3.02	15.9	2270	2.56	0.13	1.51
		9b	1.52	12.2	2100	3.18	0.05	2.06
		Unconformity	0.79	11.6	0	3.49	−0.08	2.2
		11	0.79	9.4	2030	3.9	−0.04	2.38
		12	0.49	7	1970	3.9	0.02	2.53
	Bh XVIII	6	4.47	27.2	2600	0.5	0.1	0.13
		Unconformity	4.13	23.6	0	0.91	0.12	0.36
		9a	4.13	15.9	2350	1.43	0.13	0.76
		9b	2.74	12.2	2330	2.3	0.05	1.41
		10	1.86	11.6	2150	3.29	−0.08	1.95
		11	0.95	9.4	2100	3.42	−0.04	1.94
		12	0.73	7	1970	3.82	0.02	2.34
	Bh XIV	6	3.79	23.6	2360	1.62	0.12	0.8
		8a	2.53	19.5	2330	2.31	0.14	1.19
		8b	1.86	16.5	2280	2.56	0.14	1.35
		9a	1.58	15.9	2010	3.5	0.13	2.08
		9b	0.43	12.2	1950	3.79	0.05	2.33

is based on: (1) the absence of a conspicuous load, such as a thrust sheet, that would load the elastic lithosphere, and (2) the low elastic strength of the Plato-San Jorge basin as its crust is sliced in several compartments by normal faults that would not transmit loads during extension. For eustatic corrections, we used Haq et al. (1987) sea level curve, calibrated for the Magdalena valley by Cuartas et al. (2006). The composite stratigraphic column (Fig. 5) was also backstripped following the same parameters as above.

The subsidence curves thus obtained (Fig. 6) over-estimate the amount of crustal thinning predicted, as no water-depth corrections were applied. The total tectonic subsidence is in the order of 1.5–2.5 km, with the contribution from paleobathymetry still unaccounted for. These curves, nonetheless represent a simple first-order approximation to tectonic subsidence, documenting a sharp increase in subsidence rates between 11 and 13 Ma, and slower subsidence rates for the remaining history of the basin. As with the boreholes, the stratigraphic section records an initial period of slow subsidence that increases suddenly around 12 Ma. The most stratigraphically complete boreholes in the horst areas document a time of opening of 27 Ma, which coincides with Duque-Caro's (1979) report of upper Oligocene carbonate strata directly overlying crystalline basement in the Cicuco high. Rincón et al. (2007), however, report sedimentation as old as late Eocene in one of the deep grabens of the Plato compartment (Borehole III, planktonic foraminifera zone *Subbotina yeguaensis*).

Given the over-estimation due to lack of paleobathymetric data, the amounts of crustal extension predicted here are interpreted to be the maximum values (Fig. 6, inset) obtained from backstripping the sedimentary column from boreholes and the stratigraphic section, or a beta value of less than 2.

5. Basement of the Plato-San Jorge basin

Late Permian to Early Triassic magmatic crystallization ages have been reported in the northern end of the Cordillera Central in the Puqui Complex, as well as in its eastern and western flanks (Hall et al., 1972; Ordoñez and Pimentel, 2002; Viñasco et al., 2006; Ibañez-Mejía et al., 2008). The Santa Marta massif also contains similar magmatic crystallization ages in the Sevilla province (MacDonald and Hurley, 1969; Cardona et al., this issue). The only available basement ages in the Plato-San Jorge basin to date include the ca. 110 Ma biotite K–Ar from the Cicuco-3 well (Pinson et al., 1962), and ca. 110 Ma and 60 Ma Rb–Sr, K–Ar ages from low-grade schist and a volcanic rock of the El Cabano-1 and Los Cayos-1 wells (Thery et al., 1977).

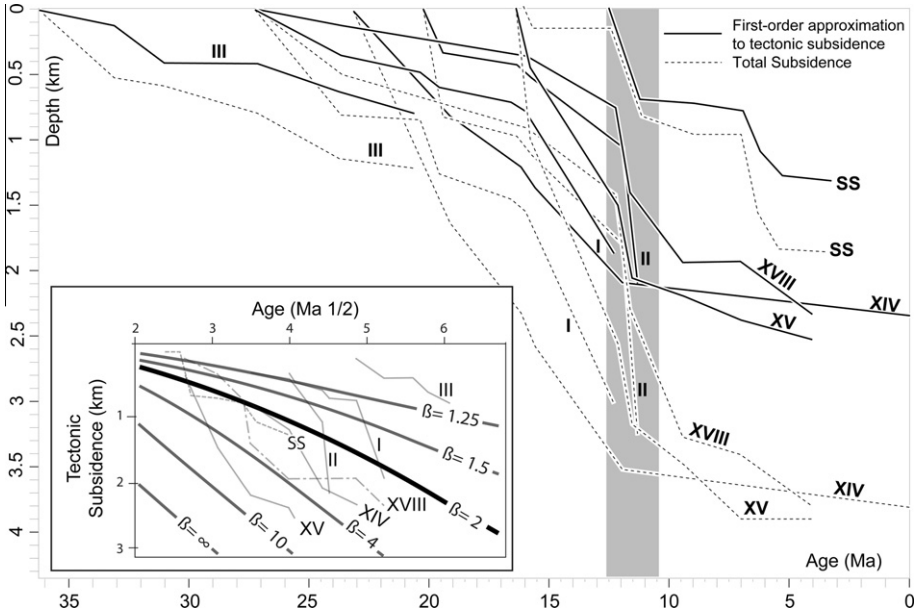

Fig. 6. First-order approximation to tectonic subsidence derived from boreholes published by Rincón et al. (2007) in roman numerals, and the stratigraphic section measured in the Carmen-Zambrano road (SS). Borehole III is the only one inside one of the deep graben areas, in the southern prong of the Plato compartment. Inset shows the first-order approximation to tectonic subsidence plotted against square root of age. The predicted value of extension is over-estimated due to insufficient water-depth data.

In order to obtain more robust geochronological constrains for the basement of the Plato-San Jorge basin, we collected samples from the Cicuco-2a, Cicuco-3 and Lobita-1 wells in the Cicuco high (Fig. 7). The rocks recovered from the Cicuco wells show a similar composition with quartz (55%), K-feldspar (15%), plagioclase (18%), biotite (6%) and muscovite (6%), while the Lobita-1 sample is a biotite granite. Fractured plagioclase and bent micas suggest some deformation at greenschist facies conditions of ca. 300° C (Passchier and Trouw, 1996). Zircons were retrieved from all samples and analyzed by the U/Pb method, which relies on the well-known strong geochronological memory of zircon and its formation during a magmatic event.

5.1. Analytical techniques

U/Pb analyses were carried out at the Arizona LASERCHRON Laboratory by Laser Ablation-Multi-Collector–ICP–Mass Spectrometry (LAM–ICP-MS). Details on the analytical procedures and description of the method are from Gehrels et al. (2006), Gehrels et al. (2008) and Valencia et al. (2006). Zircons were mounted in epoxy and polished for laser ablation analysis. The interiors of the zircon grains were ablated using a New Wave DUV193 Excimer laser (New Wave Instruments, Provo, UT, USA and Lambda Physik Inc., Ft Lauderdale, FL, USA) operating at a wavelength of 193 nm and using a spot diameter of 35 mm; laser ablation pits are ~20 μm deep. With the LA-MC-ICP-MS, the ablated material is carried via argon gas to the plasma source of a Micromass Isoprobe, which is configured in such a way that U and Pb can be measured simultaneously. Measurements were made in the static mode using Faraday collectors for ^{238}U, ^{232}Th, ^{208}Pb, ^{207}Pb, ^{206}Pb and an ion counting channel for ^{204}Pb. Analyses consist of one 20 s integration with the peak centered but no laser firing (checking background levels), and 20 1s integrations with the laser firing on the zircon grain. At the end of each analysis, a 30-s delay occurs during which time the previous sample is purged from the system and the peak signal intensity returns to background levels. The contribution of Hg to the ^{204}Pb is accounted for by subtracting the background values. Common lead corrections were made using the measured ^{204}Pb of the sample and assuming initial Pb compositions from Stacey and Krammers (1975). A fragment of a zircon crystal of known age (564 ± 4 Ma, 2s error; G.E. Gehrels, unpublished data) was analyzed after every fifth zircon analysis to correct for inter-element and Pb isotope fractionation.

Concordia ages for the three samples were calculated according to Ludwig (2003). The concordia age considers only the measurement or analytical errors. For the analyzed samples the analytical errors are 0.22% and 0.31% of the age. Other sources that contributed to the error in the final age determination are standard age, calibration correction from standard, composition of common Pb and decay constant. These uncertainties are known as the systematic error. For these samples the systematic error is 1.6%. The final error in the age of the samples is determined by adding quadratically the analytical and systematic errors. For samples Cicuco-2a and Cicuco-3 were of 1.63–1.62%, respectively. All age uncertainties are reported at the 2-sigma level.

5.2. Geochronological results

A total of 41 zircon crystals were analyzed for the Cicuco-2a granitoid sample, where tips and cores were analyzed in some of the crystals. Analyzed zircons are concordant, with 31 of them yielding a concordia age of 241.6 ± 3.9 Ma with a propagation error of 1.62%, which we relate to the magmatic age. Most of the U/Th values from this zircons are <10, as expected from their magmatic origin. Older inherited zircon cores related the genesis of this granitoid were also found, with Paleozoic, Neoproterozoic and Grenvillian ages. Similar crystallization ages were obtained from the Cicuco-3 granitoid, where 31 zircons crystals were analyzed. Nineteen grains yield a 241.6 ± 3. 9 Ma concordia age with similar propagation error of 1.63%, and older inherited Paleozoic ages were also found. This Early Triassic age is related to the magmatic age and overlaps with the Cicuco-2a granitoid age. Thirty eight zircons were analyzed from a massive biotite granite from the Lobita-1 well, adjacent to the Cicuco boreholes. Crystals show highly concordant ages and evidence of mixed and inherited ages are clearly seen in the age distribution. A major group of seventeen rims yield a concordia age of 239.6 ± 2.9 Ma. This ca. 239 Ma is similar to the crystallization ages of the Cicuco-2a and 3 granitoids, and due to

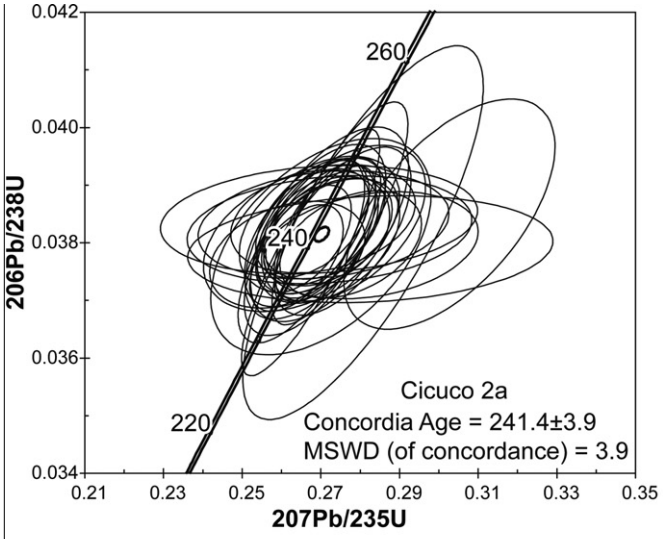

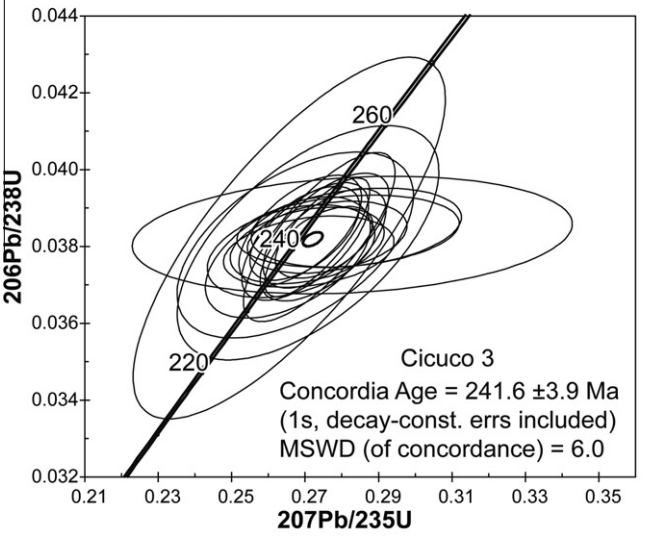

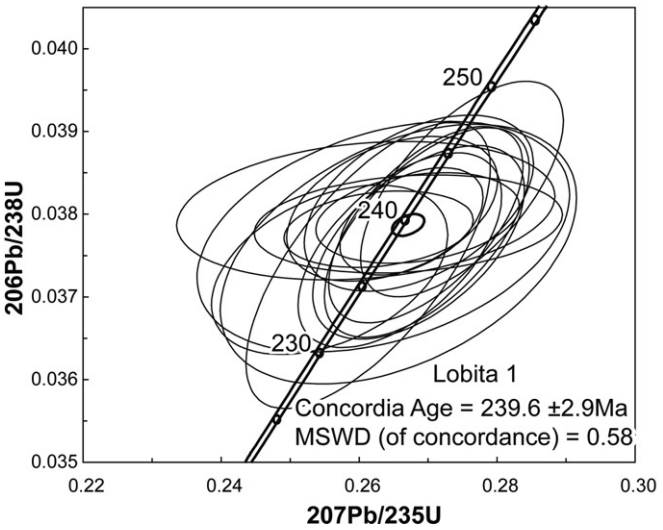

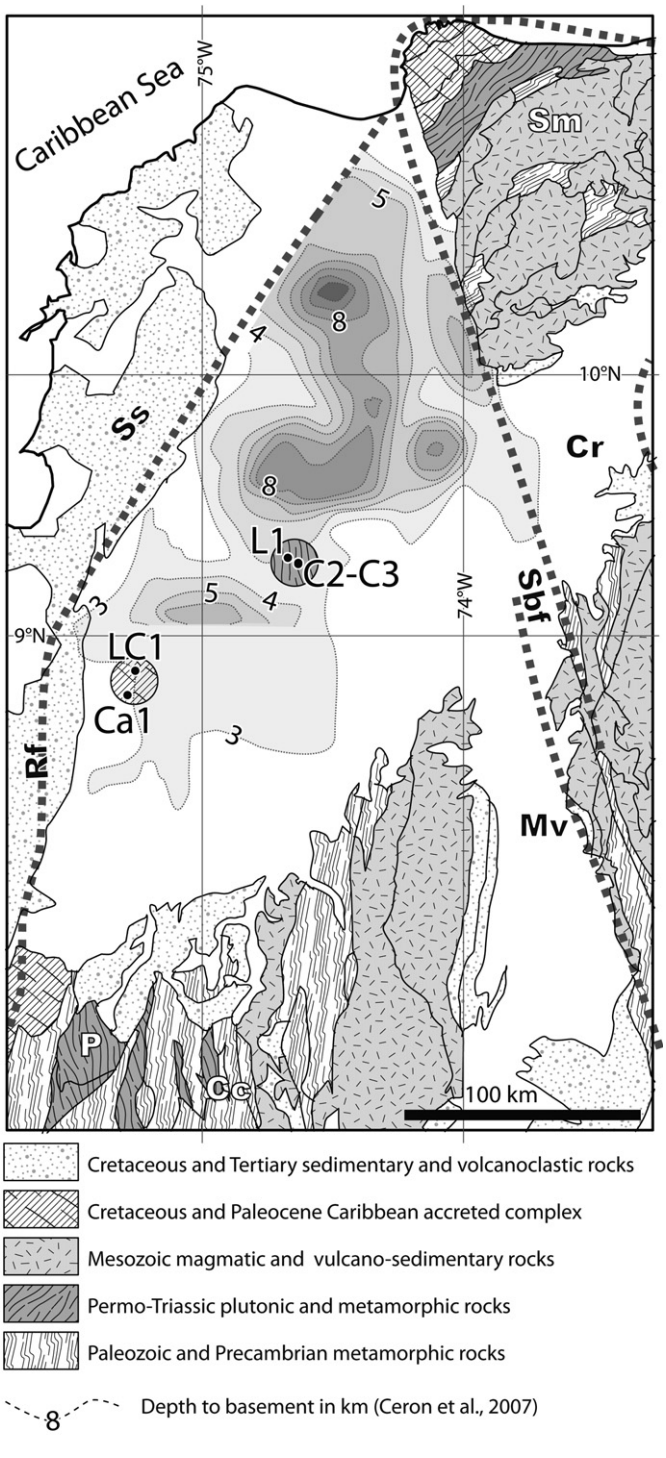

Fig. 7. Concordia plots for wells Cicuco-2a (74°38′53.07″ W, 9°16′24.781″N, 2,4 km deep), Cicuco-3 (−74°38′51.94″ W, 9°17′38.58″, 2,5 km deep) and Lobita-1 (−74°41′30.83″, 9°18′30″, 2.5 km deep). Data-point error ellipses are 2 sigma. Geologic map shows the location of the wells and other Permo-Triassic belts in the northern Cordillera Central (Ordoñez and Pimentel, 2002) and the Santa Marta massif (Cardona et al., this issue). P, Puqui complex; all other abbreviations as in Fig. 1.

their spatial proximity it suggest their geological correlation. However, six additional crystal rims show a younger 228.2 ± 2.8 Ma age, which suggest a more complex thermomagmatic evolution, which requires further exploration.

These new geochronologic data not only confirm the presence of stretched continental basement in the Plato-San Jorge basin as deduced by Cerón et al. (2007), but also constitute a new link between magmatic provinces of the same age in the Santa Marta massif (288.1 ± 4.5 and 276.5 ± 5.1 Ma, Cardona et al., this issue) and the northernmost Cordillera Central (248 ± 17 Ma, Ordoñez, 2001) through the Plato-San Jorge basin. This belt has a signature of two-mica granitoids (Viñasco et al., 2006) with a large component of inherited older crust (Ordoñez, 2001; Viñasco et al., 2006). Previous K–Ar ages in biotite of 100–110 Ma (Pinson et al., 1962) need further scrutiny, as may represent partial resetting due to a Cretaceous event (Toussaint, 1996).

6. Discussion

In the previous sections, we have presented evidence for: (1) incipient early Eocene mild deformation related to thrust sheet

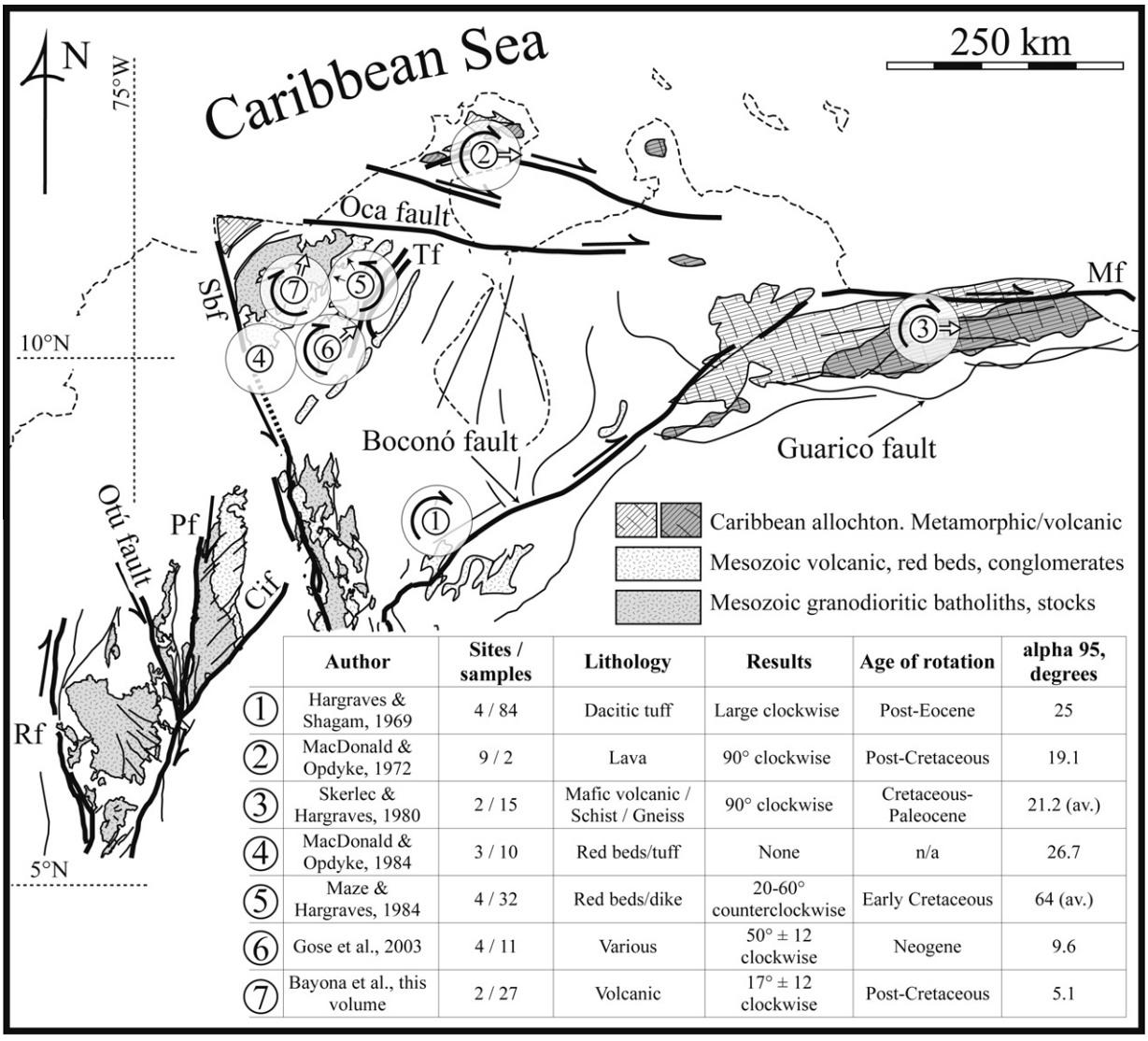

	Author	Sites / samples	Lithology	Results	Age of rotation	alpha 95, degrees
①	Hargraves & Shagam, 1969	4 / 84	Dacitic tuff	Large clockwise	Post-Eocene	25
②	MacDonald & Opdyke, 1972	9 / 2	Lava	90° clockwise	Post-Cretaceous	19.1
③	Skerlec & Hargraves, 1980	2 / 15	Mafic volcanic / Schist / Gneiss	90° clockwise	Cretaceous-Paleocene	21.2 (av.)
④	MacDonald & Opdyke, 1984	3 / 10	Red beds/tuff	None	n/a	26.7
⑤	Maze & Hargraves, 1984	4 / 32	Red beds/dike	20-60° counterclockwise	Early Cretaceous	64 (av.)
⑥	Gose et al., 2003	4 / 11	Various	50° ± 12 clockwise	Neogene	9.6
⑦	Bayona et al., this volume	2 / 27	Volcanic	17° ± 12 clockwise	Post-Cretaceous	5.1

Fig. 8. Paleomagnetic data in the northern Andes suggesting large amounts of vertical-axis rotation. α 95: half-angle of 95% confidence about the mean for sites. Cif, Cimitarra fault; Pf, Palestina fault; Tf, Tigre fault. All other abbreviations as in Fig. 1. Modified from Feininger (1970), Schubert and Sifontes (1970), Tschanz et al. (1974), Skerlec and Hargraves (1980), and Schamel (1991).

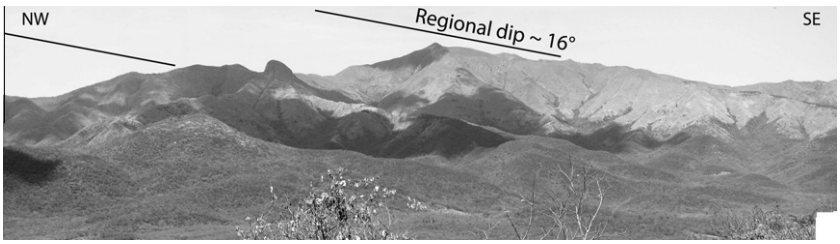

Fig. 9. Panoramic view of uniformly southeast-dipping Cretaceous and Jurassic strata along the southeastern dip-slope of the Santa Marta massif.

emplacement along the western foothills of the Perijá range; (2) late Eocene to Oligocene opening of the Plato-San Jorge basin and continued extension throughout Miocene times, and (3) a Late Permian to Early Triassic magmatic belt spanning the Cordillera Central, Santa Marta massif, and Plato-San Jorge basin. In this section we integrate this information with new and existing geophysical (Flinch, 2003; Cerón et al., 2007; Mantilla-Pimiento et al., 2009) and paleomagnetic data (Bayona et al., this issue) and present a geometric and kinematic model for the evolution of the Plato-San Jorge, Santa Marta massif and Cesar-Ranchería basin.

6.1. Paleomagnetic data

Paleomagnetic investigations in the northern Andes/southern Caribbean (Fig. 8) region suggest intermediate (50°) to large (90°) vertical-axis rotation values (Hargraves and Shagam, 1969; MacDonald and Opdyke, 1972; Skerlec and Hargraves, 1980; Gose et al., 2003). Counterclockwise vertical-axis rotations have also been also reported in the Perijá range (Maze and Hargraves, 1984), but the dispersion value reported (α-95 of 64) of these analyses is too large to be considered a reliable data point. Other paleomagnetic investigations suggest no rotation at all (Maze and Hargraves, 1984), with sampling sites near the Santa Marta–Bucaramanga fault, where local tectonic effects are likely, and may not represent the Santa Marta massif as a coherent block. More recent paleomagnetic investigations (Bayona et al., this volume) analyzed samples taken from the stable core of the Santa Marta massif, far from large faults that could generate local deformation (such as Oca and Santa Marta–Bucaramanga faults), but close enough to the Mesozoic sedimentary cover to obtain a reliable reference paleo-horizontal planes. The Ranchería river canyon, near the town of Fonseca (Fig. 2), is one of the few places meeting these conditions in the massif, with the additional advantage that construction of the Cercado dam offered fresh rock exposures in tunnels, roads and dam foundations.

Geologic maps of the Santa Marta massif (Tschanz et al., 1974) confirm that faults affecting the Mesozoic and Cenozoic rocks near the sampling site have only local significance and the results of these paleomagnetic studies can be extrapolated to the Santa Marta massif as a coherent tectonic block. Near the town of Fonseca, Cretaceous strata form resistant ridges that strongly contrast against valley-forming Paleocene strata (Jaramillo et al., 2007) of the coal-bearing Cerrejón Formation. Cretaceous and Paleocene strata uniformly dip approximately 16° to the southeast defining a simple – but regional – monocline along the southeastern flank of the Santa Marta massif (Fig. 2 and Fig. 9). Southeast-dipping volcanic and volcanoclastic Middle Jurassic rocks (Corual, Guatapurí, Los Clavos and Golero Formations) underlie Albian carbonate rocks of the Cogollo Group in angular unconformity. The Ranchería fault is the only large structure in the vicinity of the Fonseca sampling site branching out of the Cerrejón fault, and obliquely slicing the monocline with a left-lateral, strike-slip horizontal displacement in excess of 5 km duplicating the Cerrejón Formation (Fig. 2). This fault is attenuated and dissipates near Fonseca as deduced from resistant ridges of Cretaceous strata unaffected by the fault.

The magnitude of clockwise vertical-axis rotation deduced from two sites (RR2 and RR4, Bayona et al., this issue) in the Fonseca area is 17 ± 12.8° with a very low dispersion (α-95 of 5.1). Larger vertical-axis rotations were isolated in other sites near Fonseca (e.g. RR2, Bayona et al., this issue) but ignored here due poor structural control. These new paleomagnetic data lend further support to the overall vertical-axis rotation of the Santa Marta massif, but with moderate values, instead of intermediate to large values found in the southern Caribbean region (Hargraves and Shagam, 1969; MacDonald and Opdyke, 1984; Skerlec and Hargraves, 1980; Gose et al., 2003). The discrepancy in the magnitude of rotation needs to be investigated further.

6.2. Structure

Structure of the Plato-San Jorge basin is reinterpreted here from three main sources: Cerón et al. (2007) comprehensive geophysical analysis, and Flinch's (2003) and Mantilla-Pimiento's (2009) seismic sections. Geophysical information is complemented with published boreholes (Rincón et al., 2007) to control depth to basement. Two seismic sections and line-drawings of seismic sections

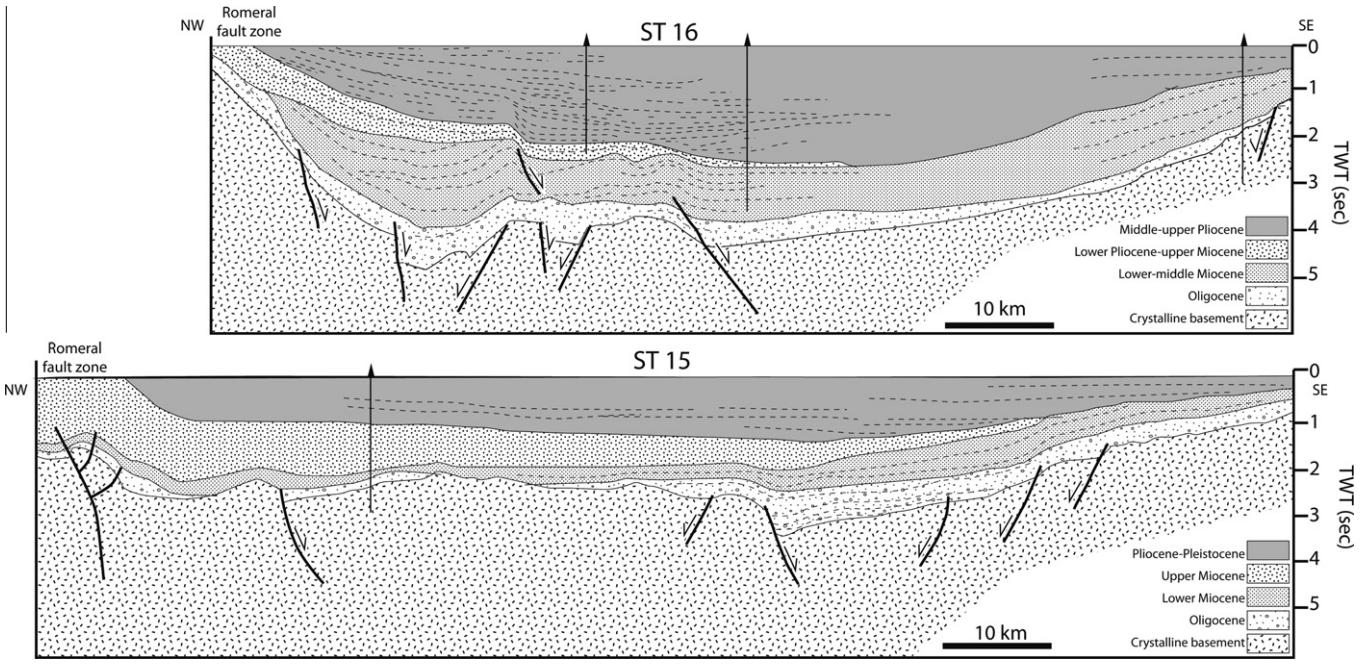

Fig. 10. Line-drawings from seismic sections reinterpreted from those published by Flinch (2003) for the southern part of the Plato-San Jorge basin. Seismic transect 16 (ST16) and 15 (ST15).

presented by Flinch (2003) and Mantilla-Pimiento et al. (2009) were reinterpreted, while geophysically derived basement contours (Cerón et al., 2007) were re-drawn in light of the structural style of graben and horsts defined in the seismic sections (Fig. 10).

Uninterpreted seismic sections published by Flinch (2003) and Mantilla-Pimiento et al. (2009), display a mostly undeformed, flat-lying sedimentary sequence where strong seismic reflectors define normal faults in grabens that preserve a sedimentary package as old as Oligocene, with faults crossing strata as young as upper Miocene. A thick Pliocene to Pleistocene package blankets the entire basin. The crystalline basement approaches the surface towards the northwestern edge of the basin, where reactivation and deformation related to the Romeral fault zone has exposed strata as old as Miocene (Fig. 5). Only a few of the faults depicted in the seismic transects of Flinch (2003) and Mantilla-Pimiento et al. (2009) could be incorporated in the final reinterpretation (Fig. 11) as the spatial resolution of this data set is much larger than Cerón's et al. (2007) geophysically derived basement contours.

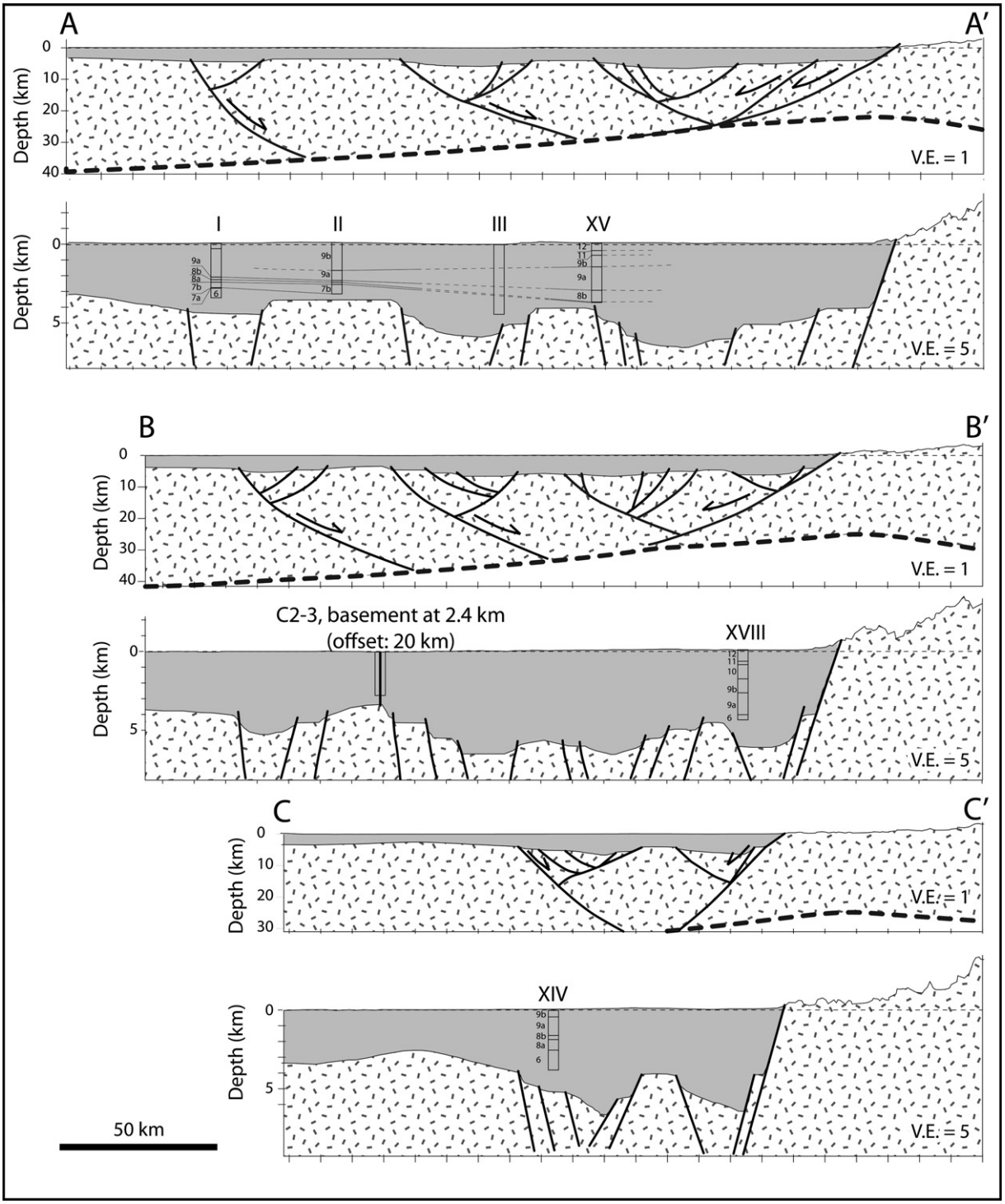

Fig. 11. Cross-sections across Plato-San Jorge basin illustrating the structural style interpreted on the basis of published geophysical information (Flinch, 2003; Cerón et al., 2007) and borehole data (Rincón et al., 2007).

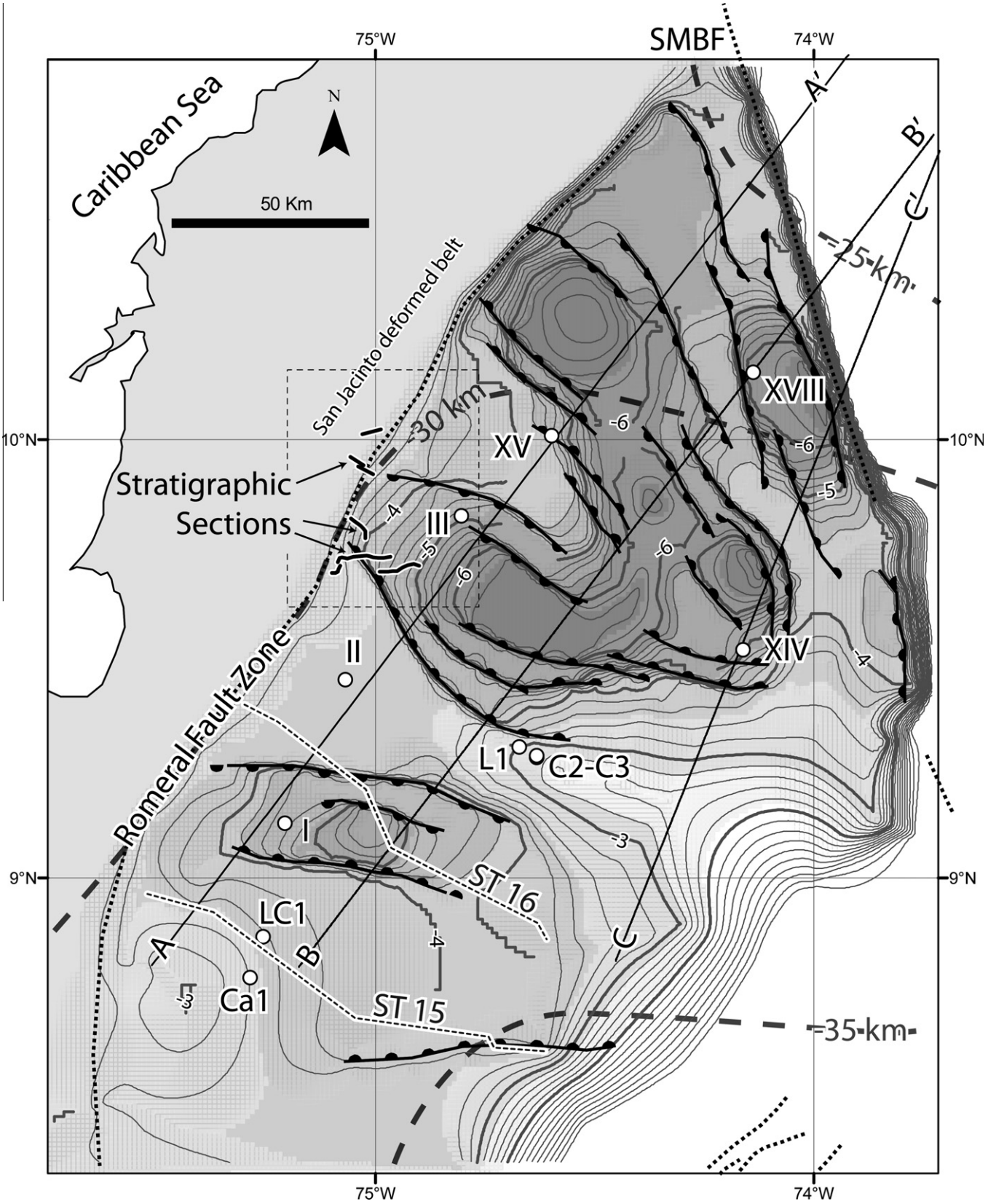

Fig. 12. Basement map of the Plato-San Jorge basin reinterpreted from Cerón et al. (2007) incorporating normal faults to bound the main basement depressions. Thick dashed line indicates depth to Moho (Cerón et al., 2007). Roman numerals indicate location of boreholes published by Rincón et al. (2007), ST15 and ST16 represent seismic transects published by Flinch (2003). Location of profiles AA′, BB′, and CC′indicated by solid lines. Abbreviations as in Fig. 1.

Cross-sections were drawn perpendicular to major structures (Fig. 11) where borehole information from Rincón et al. (2007) was projected to constrain structure and depths to basement. These sections illustrate basin geometry in agreement with available geophysical and borehole information, where normal faults should accommodate the tectonic contribution of the crustal

stretching calculated from first-order tectonic subsidence analysis (beta of approximately 2, Fig. 6). The resulting picture (Fig. 12) reveals a nearly 200 km-wide, fan-shaped, sedimentary basin filled with upper Eocene to Oligocene and younger strata, sitting on extended continental crust in three compartments: El Dificil, a deep and elongated, NNW-trending basin with 6 km of sediment fill; Plato, a two-prong, NW-trending extensional basin with up to 6 km of sediment fill; and San Jorge, a single WNW-trending extensional basin, with up to 5 km of sediment fill. The latter two subbasins are separated by the Cicuco horst, a WNW-trending basement high with 2–3 km of sediment cover. Together, these structural features define a fan-like arrangement of normal faults from nearly westerly trends in the south (San Jorge basin) to more northerly-trending structures closer to the Santa Marta massif with an apex to the southeast.

6.3. Geometric model

For the construction of the model we sought to obtain an original geometry that would close most of the graben areas defined in Fig. 12. Best-fit closure was used as the initial stage to calculate kinematic estimates along the Santa Marta–Bucaramanga, Oca and Cerrejón faults, as well as for the normal faults in the Plato-San Jorge basin. We assumed that the horst areas (shades of grey in Fig. 13) remain constant and behave rigidly, while the deep grabens (white in Fig. 13) were allowed to distort accommodating much of the extension. The northern Cordillera Central and the Maracaibo block remain fixed, and the rotating Santa Massif was modeled as a rigid block fully detached from the Perijá range. This model ignores any partition of deformation that may have occurred within the Perijá range, where strike-slip structures such as the Tigre fault may take up part of the deformation assigned here exclusively to the Cerrejón fault. Euler poles and rotation values (Table 2) were solely derived from the best-fit closure constraint, and calculated for each one of the rigid blocks.

The tectonic model presented here (Fig. 13) considers two simple scenarios: the first one with a clockwise, vertical-axis rotation value for the Santa Marta massif of 30°, achieving a nearly complete closure of graben areas, and a second one with a clockwise rotation value of 23°. In both cases, clockwise, vertical-axis rotation of the Santa Marta massif predicts that the displacement along the Cerrejón fault, and all the structures sharing this oblique contraction (e.g. Tigre and Motilones faults), would decrease to the southwest along strike from a maximum at its northeastern tip. Vertical-axis rotation of the Santa Marta massif would also predict a left-lateral slip for the Oca fault relative to a stationary Caribbean plate, but a right-lateral slip is necessarily derived relative to a far-travelled Caribbean plate (Pindell et al., 1998; Kennan and Pindell, in press), and further predicts that most of the displacement observed on the Oca fault may be the result of shortening along the Perijá range as previously noted by Kellogg (1984). The left-lateral Santa Marta Bucaramanga fault would have a maximum displacement near its northernmost tip and decreasing along the strike to the south. A rotating Santa Marta massif also predicts that extension in the fan-shaped Plato-San Jorge basin would have a maximum value along its northwestern edge and would decrease to a minimum towards its southeastern apex. Both scenarios depict an undeformed stage that would represent a micro-plate configuration valid for the middle to late Eocene (Fig. 14) as deformation – both contractional and extensional – was beginning to be recorded in the Cesar-Ranchería and Plato-San Jorge basins, respectively.

Given a 23° vertical-axis rotation of the Santa Marta massif, the amount of lithospheric stretching derived from this geometric model is 1.47 in the Plato-San Jorge basin and about 50 km of shortening for the Perijá range with an angular shear of 0.42, about

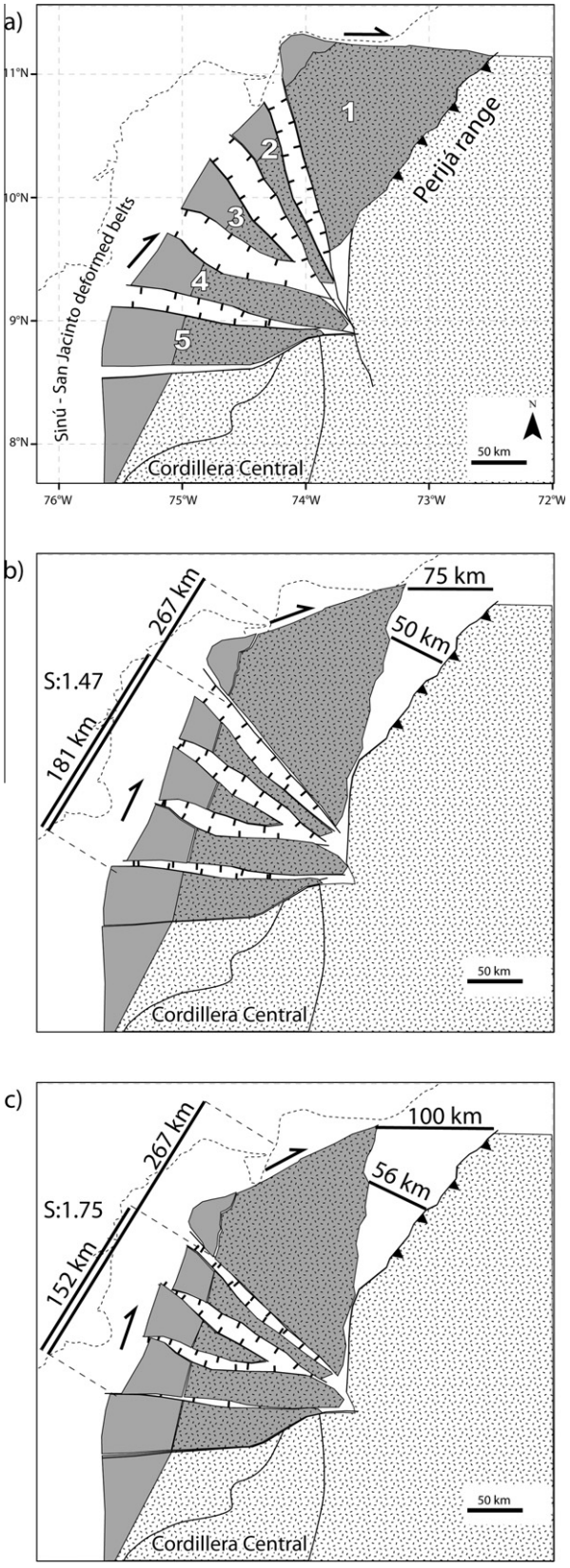

Fig. 13. Tectonic model for the simultaneous rotation of the Santa Marta massif, opening of the Plato-San Jorge basin along its trailing edge, and shortening of the Cesar-Ranchería basin along its leading edge. (A) Present configuration, (B) 23° of clockwise, vertical-axis rotation of the Santa Marta massif, and (C) 30° of clockwise, vertical-axis rotation of the Santa Marta massif. Stretching values calculated for the northwesternmost Plato-San Jorge basin. Shortening estimates along the Cerrejón fault represent a consolidated figure for all the faults in the Perijá range, including the Motilones and the Tigre fault, where strain partitioning probably took place.

Table 2
Model data.

Plate	23° Case			30° Case		
	Euler pole		Rotation magnitude	Euler pole		Rotation magnitude
	Latitude	Longitude		Latitude	Longitude	
1	9.6	−73.22	23	9.51	−73.05	30
2	9.3	−73.75	23	9.25	−73.55	28
3	9.06	−73.7	14	8.66	−73.59	16
4	8.87	−73.82	8	8.59	−73.50	8
5	8.5	−73.77	3	8.50	−73.77	3

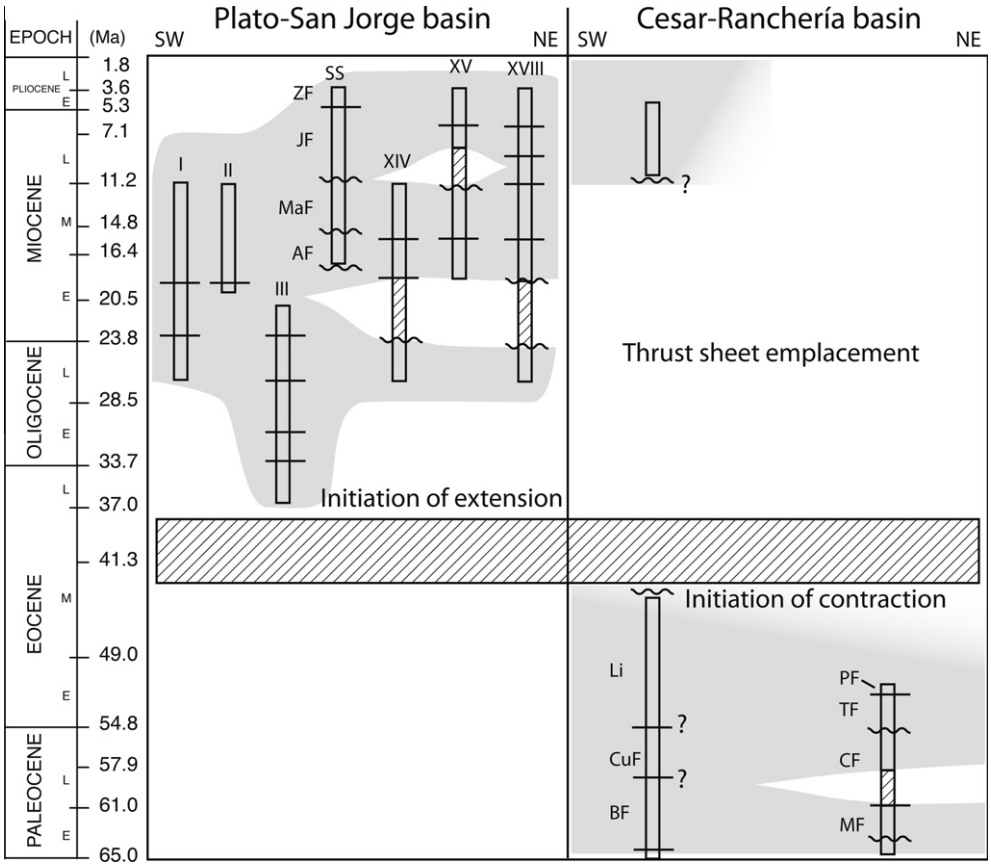

Fig. 14. Tectonostratigraphic diagram of the basins on both sides of the Santa Marta massif. Borehole III constrains the earliest opening age for the Plato-San Jorge basin, along southern prong of the Plato compartment. Li: La Loma informal unit, CuF: Cuervos Fm., PF: Palmito Fm., TF: Tabaco Fm., CF: Cerrejón Fm., MF: Manatial Fm., SS: Stratigraphic section of figure 5, ZF: Zambrano Fm., JF: Jesús del Monte Fm., MaF: Mandatú Fm, AF: Alférez Fm. (Stratigraphic columns after Rincón et al., 2007; Bayona et al., 2007; Guzmán, 2007; Ayala, 2009).

40 km of left-lateral displacement for the Santa Marta–Bucaramanga fault and an amount of right-lateral displacement along the Oca fault of 75 km. For a 30° vertical-axis rotation of the Santa Marta massif, the amount of lithospheric stretching derived for the Plato-San Jorge basin is 1.75, with about 56 km of shortening for the Perijá range, angular shear of 0.57, 45 km of left-lateral displacement along the Santa Marta–Bucaramanga fault and 100 km of right-lateral displacement along the Oca fault (Fig. 13).

Extensional values derived for the Plato-San Jorge basin (beta values between1.47 and 1.75; 86 and 115 km, respectively) agree with first-order estimates of lithospheric stretching estimates derived from borehole data (beta values of less than 2). Estimates of slip derived for the Oca fault east of Perijá (75–100 km, Fig. 13) similarly agree well with published data (90 ± 8 km, Kellogg, 1984). Combined shortening estimates for the Perijá range (50–56 km, Fig. 13) fall within the same range as combined shortening along the Cerrejón, Tigre, Guasare, Mostrencos arch faults (25–35 km, Kellogg, 1984), and Tigre fault (7–11 km, Kellogg, 1984). Left-lateral slip derived for the Santa Marta–Bucaramanga fault (40–45 km) is about half of previous estimates (110 km, Campbell, 1965) because previous estimates assumed that all deformation was focused along the fault, whereas the value derived here is just the north-south component of the deformation, where total northeast-southwest extension in the Plato-San Jorge basin is between 86 and 115 km with a total north-south component of 72–94 km, respectively.

7. Conclusions

A new geometric model explaining the simultaneous extensional and contractional deformation in the Plato-San Jorge and Cesar-Ranchería basins adequately explains the simultaneous, yet contrasting, structural styles found on two of the flanks of the Santa Marta massif. New structural mapping documents that Eocene

and younger shortening took place along the western foothills of the Perijá range while stratigraphic sections measured in the western edge of the Plato basin and existing biostratigraphic zonations based on industry borehole information (Rincón et al., 2007; Cuartas et al., 2006) record post- late Eocene basin opening and extension in the Plato-San Jorge basin. The resulting palinspastic model suggests that even moderate amounts (30°) of vertical-axis, clockwise rotation of the Santa Marta massif can simultaneously solve approximately 115 km of extension along its trailing edge (Plato-San Jorge basin) and about 100 km of right-lateral shear along its leading edge (Perijá range). Extension in the Plato-San Jorge basin would have segmented a once continuous Permo-Triassic magmatic belt spanning the Santa Marta massif, the Plato-San Jorge basin and the northern Cordillera Central. The amount of lithospheric stretching derived for the Plato-San Jorge basin is between 1.75 and 2, with about 56 km of shortening predicted for the Perijá range with an angular shear of 0.57. Only 45 km of left-lateral displacement is derived for the Santa Marta–Bucaramanga fault and 100 km of right-lateral displacement for the Oca fault (Fig. 13).

This model explains the magnitudes, styles and timing of deformation, thus placing additional constraints on the possible paleogeographic configurations of this margin, as a simultaneously extending Plato-San Jorge basin and contracting Cesar-Ranchería basin would strongly affect paleodrainage and facies distributions. This palinspastic restoration is a tool to analyze facies distributions and paleodrainage patterns to better predict distributions of source areas and reservoir rocks in northern Colombia. Additional paleomagnetic investigations as well as detailed provenance analyses are needed to further our understanding of the dynamics of this complex margin.

Acknowledgements

Banco de la República de Colombia partially funded analytical data, Project 2289. Funding for the Arizona LaserChron Center is provided by NSF EAR-0443387. This is a contribution to the IGCP 546: ‘‘Subduction zones of the Caribbean”. Carbones del Cerrejón Ltd., provided support to students mapping the northern part of the Cesar-Ranchería valley. Thanks to I. Gutierrez for help in field expeditions, to G. Ojeda and C. Vargas for core sampling at the Litoteca Nacional and to N. Hoyos for help in the reconstructions. Backstrip OSX, and Gplates were used in this paper. Comprehensive reviews by F. Roure and an anonymous reviewer helped improve the quality of the manuscript, the authors, however, remain responsible for all errors of fact and interpretation.

References

Ayala, C., 2009. Análisis tectonoestratigráfico y de procedencia en la subcuenca del Cesar: relación con los sistemas petroleros. M.Sc. thesis, Universidad Simón Bolivar, Venezuela, 183 pp.

Bayona, G.A., Lamus-Ochoa, F., Cardona, A., Jaramillo, C.A., Montes, C., Tcheglilakova, N., 2007. Procesos orogénicos del Paleoceno para la cuenca de Ranchería (Guajira, Colombia) y áreas adyacentes definidos por análisis de procedencia. Geología Colombiana 32, 21–46.

Bayona, G., Jimenez, G., Silva, C., Cardona, A., Montes, C., Roncancio, J., this issue. Paleomagnetic data uncovered from Mesozoic units of the Santa Marta Massif: constrain for paleogeographic and paleotectonic evolution of the NW corner of the South America plate. Journal of South American Earth Sciences: Special Volume Sierra Nevada de Santa Marta.

Burke, K., Fox, P.J., Sengör, A.M.C., 1978. Buoyant ocean floor and the evolution of the Caribbean. Journal of Geophysical Research 83, 3949–3954.

Burke, K., Cooper, C., Dewey, J., F., Mann, P., Pindell, J.L., 1984. Caribbean tectonics and relative plate motions. In: Bonini, W.E., Hargraves, R.B., Shagam, R. (Eds.), The Caribbean–South American Plate Boundary and Regional Tectonics, GSA Memoir, vol. 162. Boulder, CO, United States, pp. 31–63.

Campbell, C.J., 1965, The Santa Marta wrench fault of Colombia and its regional setting. In: Saunders, J.B. (Ed.), Transactions of the Fourth Caribbean Geological Conference. Port-of-Spain, pp. 247–262.

Cardona, A., Valencia, V., Bayona, G., Duque, J., Gehrels, G., Jaramillo, C.A., Montes, C., Ojeda, G.A., Ruiz, J., in press. Turonian to Eocene accretion and subduction in the Santa Marta massif and Ranchería basin. In: Implications for northern Andean Orogeny: Geology, Colombia.

Cardona, A., Ruiz, J., Valencia, V., Garzón, A., Ojeda, G., Weber, M., this issue. Early Permian plutonism in the northeast Sierra Nevada de Santa Marta, Colombian–Caribbean region: tectonic setting and paleogeographic implications within Pangea configuration. Journal of South American Earth Sciences: Special Volume Sierra Nevada de Santa Marta.

Cediel, F., Shaw, R.P., Caceres, C., 2003. Tectonic assembly of the Northern Andean Block. In: Bartolini, C., Buffler, R.T., Blickwede, J. (Eds.), The Circum-Gulf of Mexico and the Caribbean: Hydrocarbon Habitats, Basin Formation, and Plate Tectonics, vol. 79. AAPG Memoir, pp. 815–848.

Cerón, J.F., Kellogg, J.N., Ojeda, G.Y., 2007. Basement configuration of the northwestern South America–Caribbean margin from recent geophysical data. Ciencia, Tecnología y Futuro 3, 25–49.

Cuartas, C., Jaramillo, C.A., Martinez, J.I., 2006. Quantitative biostratigraphic model for the tertiary of the lower Magdalena basin, Colombian Caribbean. Ciencia, Tecnología y Futuro 3, 7–28.

DePorta, J., 1962. Consideraciones sobre el estado actual de la estraigrafía del Terciario de Colombia. Boletín de Geología de la Universidad Industrial de Santander 9, 5–43.

Duerto, L., Escalona, A., Mann, P., 2006. Deep Structure of the Mérida Andes and Sierra de Perijá Mountain Fronts, AAPG Bulletin, vol. 90. Maracaibo basin, Venezuela (pp. 505–528).

Duque-Caro, H., 1975. Los foraminiferos planctónicos y el Terciario de Colombia. Revista Española de Micropaleontología 7 (3), 403–427.

Duque-Caro, H., 1979. Major structural elements and evolution of northwestern Colombia. In: Watkins, J.S., Montadert, L., Dickerson, P.W. (Eds.), Geological and Geophysical Investigations of Continental Margins: AAPG Memoir, vol. 29, pp. 329–351.

Espitia, W., 2008, Cartografía geológica con énfasis estructural en la zona este de Barrancón. Undergraduate Thesis, Universidad Nacional de Colombia, Bogota, 20 pp.

Feininger, T., 1970. The Palestina Fault, GSA Bulletin, vol. 81. Colombia (pp. 1201–1216).

Flinch, J.F., 2003. Structural evolution of the Sinú-Lower Magdalena area (northern Colombia). In: Bartolini, C., Buffler, R.T., Blickwede, J. (Eds.), The Circum-Gulf of Mexico and the Caribbean: Hydrocarbon Habitats, Basin Formation, and Plate Tectonics, AAPG Memoir, vol. 79, pp. 776–796.

Gehrels, G., Valencia, V., Pullen, A., 2006. Detrital zircon geochronology by Laser-Ablation Multicollector ICPMS at the Arizona LaserChron Center. In: Olszewski, T.D. (Ed.), Geochronology Emerging Opportunities, vol. 12. Paleontological Society, pp. 67–76.

Gehrels, G., Valencia, V., Ruiz, J., 2008. Enhanced precision, accuracy, efficiency, and spatial resolution of U-Pb ages by laser ablation–multicollector-inductively coupled plasma–mass spectrometry. Geochemistry Geophisics Geosystems, doi:10.1029/2007GC001805.

Gómez, E., Jordan, T.E., Allmendinger, R.W., Hegarty, K., Kelley, S., 2005. Syntectonic Cenozoic Sedimentation in the Northern Middle Magdalena Valley and Implications for Exhumation of the Northern Andes, Geological Society of America Bulletin, vol. 117 (pp. 547–569).

Gose, W.A., Perarnau, A., Castillo, J., 2003. Paleomagnetic results from the Perija Mountains, Venezuela: an example of vertical axis rotation. In: Bartolini, C., Buffler, R.T., Blickwede, J. (Eds.), The Circum-Gulf of Mexico and the Caribbean: Hydro-Carbon Habitats, Basin Formation and Plate Tectonics. AAPG Memoir, vol. 79, pp. 969–997.

Guzmán, G., 2007. Stratigraphy and Sedimentary Environment and Implications in the Plato Basin and the San Jacinto Belt, Northwestern Colombia. Ph.D. Thesis, University of Liége, Belgium, 275 pp.

Hall, R.B., Álvarez, J., Rico, H., 1972. Geología de parte de los departamentos de Antioquia y Caldas (Subzona II-A), Boletín Geológico Ingeominas, vol. 20, pp. 1–85.

Haq, B.U., Hardenbol, J., Vail, P.R., 1987. Chronology of fluctuating sea levels since the Triassic (250 million years ago to present). Science 235, 1156–1167.

Hargraves, R.B., Shagam, R., 1969. Paleomagnetic study of La Quinta Formation, Venezuela. American Association of Petroleum Geologists Bulletin 53, 537–552.

Hernandez, R., Ramirez, V., 2003. Rotacion tectónica del noroeste de Sur América vs patrones de fracturamiento. In: Resúmenes del IX Congreso Colombiano de Geología, Medellín, pp. 19–21.

Hernandez, R., Ramirez, V., Reyes, J. P., 2003. Evolución geohistórica de las cuencas del norte de Colombia. In: Resúmenes del VIII Simposio Bolivariano de Exploración en las Cuencas Subandinas, pp. 256–258.

Ibañez-Mejía, M., Jaramillo-Mejía, J.M., Valencia, V., 2008. U-Th/Pb zircon geochronology by multicollector LA-ICP-MS of the Samaná Gneiss: a Middle Triassic syn-tectonic body in the Central Andes of Colombia, related to the latter stages of Pangea assembly. In: VI South American Symposium on Isotope Geology San Carlos de Bariloche – Argentina (extended abstract).

Irving, E.M.,1971. Structural Evolution of the Northernmost Andeas, Colombia. USGS Professional Paper 846, Washington DC, 27 pp.

Jaramillo, C., Bayona, G., Pardo-Trujillo, A., Rueda, M., Torres, V., Harrington, G., Mora, G., 2007. The Palynology of the Cerrejón Formation (Upper Paleocene) of Northern Colombia. Palynology 31, 153–189.

Jaramillo, C., et al., in press. Biostratigraphy breaking paradigms: dating the Mirador Formation in the Llanos Basin of Colombia. In: Demchuck, T. (Ed.), Geological Problem Solving with Microfossils. SEPM Special Publication, Tulsa, OK.

Kellogg, J., 1984. Cenozoic and tectonic history of the Sierra de Perijá, Venezuela-Colombia, and adjacent basins. GSA Memoir 162, 239–261.

Kellogg, J.N., Bonini, W.E., 1982. Subduction of the Caribbean plate and basement uplifts in the overriding South American plate. Tectonics 1, 251–276.
Kennan L., and Pindell J., in press. Dextral shear, terrane accretion and basin formation in the northern Andes: best explained by interaction with a Pacific-derived Caribbean plate. In: James, K., Lorente, M.A., Pindell, J. (Eds.), The Geology and Evolution of the Region between North and South America. Geological Society of London (special publication).
Ludwig, K.J., 2003. Isoplot 3.0: Berkeley Geochronology Center Special Publication, No. 4, 70 pp.
MacDonald, W.D., Hurley, P.M., 1969. Precambrian gneisses from northern Colombia, South America. Geological Society of America Bulletin 80, 1867–1872.
MacDonald, W.D., Opdyke, N.D., 1972. Tectonic rotations suggested by paleomagnetic results from Northern Colombia, South America. Journal of Geophysical Research 77, 5720–5730.
MacDonald, W.D., Opdyke, N.D., 1984. Preliminary paleomagnetic results from Jurassic rocks of the Santa Marta massif, Colombia. In: Bonini, W.E., Hargraves, R.B., Shagam, R. (Eds.), The Caribbean–South American Plate Boundary and Regional Tectonics, GSA Memoir, vol. 162, pp. 295–298.
Mann, P., Burke, K., 1984. Neotectonics of the Caribbean. Review of Geophysics and Space Physics 22, 309–362.
Mantilla-Pimiento, A., Jentzsch, G., Kley, J., Alfonso-Pava, C., 2009. Configuration of the Colombian Caribbean margin: constraints from 2D seismic reflection and potential fields interpretation. In: Lallemand, S., Funicello, F. (Eds.), Subduction Zone Geodynamics. Berlin, pp. 247–272.
Maze, W.B., Hargraves, R.B., 1984. Paleomagnetic results from the Jurassic La Quinta Formation in the Perijá Range, Venezuela, and their tectonic significance. In: Bonini, W.E., Hargraves, R.B., Shagam, R. (Eds.), The Caribbean–South American Plate Boundary and Regional Tectonics, GSA Memoir, vol. 162, pp. 287–293.
McKenzie, D., 1978. Some remarks on the development of sedimentary basins. Earth and Planetary Science Letters 40, 25–32.
Montes, C., 2003. Oblique convergence and rotations derived from the kinematics of the Piedras-Girardot area, Colombia. In: Resúmenes del IX Congreso Colombiano de Geología, Medellín, pp. 18–19.
Montes, C., Hatcher Jr., R.D., Restrepo, P.A., 2005a. Tectonic reconstruction of the northern Andean blocks: oblique convergence and rotations derived from the kinematics of the Piedras-Girardot area, Colombia. Tectonophysics 399, 221–250.
Montes, C., Bayona, G., Jaramillo, C., Ojeda, G., Molina, M., Herrera, F., 2005b, Uplift of the Sierra Nevada de Santa Marta and Subsidence in the Cesar-Rancheria Valley: Rigid-Beam Pivot Model. In: Extended Abstracts, Sixth International Symposium of Andean Geodynamics, pp. 520–523.
Moreno-Sánchez, M., Pardo-Trujillo, A., 2003, Stratigraphical and sedimentological constraints on western Colombia: Implications on the evolution of the Caribbean plate. In: Bartolini, C., Buffler, R.T., Blickwede, J. (Eds.), The Circum-Gulf of Mexico and the Caribbean: Hydro-Carbon Habitats, Basin Formation and Plate Tectonics, AAPG Memoir, vol. 79, pp. 891–892.
Muller, J., Di Giacomo, E., Van Erve, A., 1987. A palynologic zonation for the cretaceous, tertiary and quaternary of northern South America. American Association of Stratigraphic Palynologists Contribution Series 19, 7–76.
Olivella, A., 2005. Cartografía geológica del tajo La Puente, Carbones del Cerrejón. Undergraduate Thesis, Universidad Pedagógica y Tecnológica de Sogamoso, 84 pp.
Ordoñez, O., 2001. Caracterização isotópica Rb–Sr e Sm–Nd dos principais eventos magmáticos nos Andes Colombianos. Tesse de Doutoramento Universidade de Brasilia, 197 pp.
Ordoñez, O., Pimentel, M., 2002. Rb–Sr and Sm–Nd isotopic study of the Puqui complex, Colombian Andes. Journal of South American Earth Sciences 15 (2), 173–182.
Palencia, A., 2007. Análisis estructural y geométrico del anticlinal de Tabaco en la mina del Cerrejón, Guajira. Undergraduate Thesis, Universidad EAFIT, 108 pp.
Passchier, C.W., Trouw, R.A., 1996. Microtectonics. Springer, 288 pp.
Petters, V., Sarmiento, R., 1956. Oligocene and lower Miocene biostratigraphy of the Carmen-Zambrano area, Colombia. Micropaleontology 14, 7–35.
Pindell, J.L., Kennan, L., 2001, Kinematic evolution of the Gulf of Mexico and Caribbean. Transactions, Petroleum systems of deep-water basins: global and Gulf of Mexico experience. In: GCSSEPM 1st Annual Research Conference. Houston, Texas, G CSSEPM, pp. 159–192.
Pindell, J.L., Higgs, R., Dewey, J.F., 1998. Cenozoic palinspastic reconstruction, paleogeographic evolution and hydrocarbon setting of the northern margin of South America. In: Pindell, J.L., C. Drake, L. (Eds.), Paleogeographic Evolution and Non-glacial Eustasy, northern South America. SEPM, Tulsa, pp. 45–85 (special publication).
Pinson, W.H., Hurley, P.M., Mencher, E., Fairbairn, H.W., 1962. K–Ar and Rb–Sr ages of biotites from Colombia, South America. Geological Society of America Bulletin 73, 907–910.
Reyes, J.P., Mantilla, M., Gonzalez, J.S., 2000. Regiones tectono-sedimentarias del valle inferior del Magdalena, Colombia. In: Resúmenes de la Primera Convención Técnica de la A.C.G.G.P.
Rincón, D., Arenas, J.E., Cuartas, C.H., Cárdenas, A.L., Molinares, C.E., Caicedo, C., Jaramillo, C., 2007. Eoocene–Pliocene planktonic foraminifera biostratigraphy from the continental margin of the southwest Caribbean. Stratigraphy 4, 261–311.
Ruiz, M.C., 2006, Cartografía estructural del flanco occidental del anticlinal del tajo Tabaco Uno en la mina de Carbones del Cerrejón. Undergraduate Thesis, Universidad Nacional de Colombia, Medellin, 78 pp.
Sánchez, C.A., 2008. Exploración geológica del pit Annex y las zonas circundantes en el piedemonte de la Serranía del Perijá. Undergraduate Thesis, Universidad Nacional de Medellin, 48 pp.
Schamel, S., 1991. Middle and upper Magdalena basins, Colombia. In: Biddle, K.T. (Ed.), Active Margin Basins, AAPG Memoir, vol. 52. Tulsa, OK, United States, pp. 283–301.
Schubert, C., Sifontes, R.S., 1970. Bocono fault, Venezuelan Andes: evidence of postglacial movement. Science 170 (3953), 66–69.
Skerlec, G.M., Hargraves, R.B., 1980. Tectonic significance of paleomagnetic data from northern Venezuela. Journal of Geophysical Research 85 (B10), 5303–5315.
Stacey, J.S., Krammers, J.D., 1975. Approximation of terrestrial lead isotope evolution by a two stage model. Earth and Planetary Science Letters 26, 207–221.
Stone, B., 1968. Planktonic foraminiferal zonation in the Carmen-Zambrano area, Colombia. Micropaleontology 14, 363–364.
Thery, J.-E., Esquevin, J., Menendez, R., 1977. Signification géotectonique de datations radiométriques dans des sondages de Basse Magdalena (Colombie). Bulletin des Centres de Recherches Exploration-Production Elf-Aquitaine 1, 475–494.
Toussaint, J.F., 1996. Evolución geológica de Colombia. Cretácico Universidad Nacional de Colombia, Medellín (277 pp).
Tschanz, C., Marvin, R., Cruz, J., Mennert, H., Cebula, E., 1974. Geologic evolution of the Sierra Nevada de Santa Marta. Geological Society of America Bulletin 85, 269–276.
Valencia, V.A., Noguez-Alcantara Benito, Barra, F., Ruiz, J., Gehrels, G., Quintanar, F., Valencia-Moreno, M., 2006. Re–Os Molybdenite and LA–ICPMS U–Pb zircon geochronology from the milpillas porphyry copper deposit: insights for mineralization in the Cananea District, Sonora, Mexico. Revista Mexicana de Ciencias Geológicas 23, 39–53.
Villamil, T., 1999. Campanian–Miocene tectonostratigraphy, depocenter evolution and basin development of Colombia and western Venezuela: Palaeogeography, Palaeoclimatology. Palaeoecology 153 (1–4), 239–275.
Viñasco, C.J., Cordani, U.G., González, Weber, M., Pelaez, C., 2006. Geochronological, isotopic and geochemical data from Permo-Triassic granitic gneisses and granitoids of the Colombian Central Andes. Journal of South American Earth Sciences 21, 355–371.